Experimental Investigation of Contamination and Adhesion Failure of Type II Aircraft Ground De-Icing Fluids

by

Susanne Schroll

B.S., Aerospace Engineering
Florida Institute of Technology , June 1994

Submitted to the Department of Aeronautics and Astronautics in
Partial Fulfillment of the Requirements for the Degree of

MASTER OF SCIENCE
in Aeronautics and Astronautics
at the

Massachusetts Institute of Technology

September 1995

Signature of Author _____
Department of Aeronautics and Astronautics
August 14, 1995

Certified by _____
Robert John Hansman, Jr.
Professor of Aeronautics and Astronautics
Thesis Supervisor

Accepted by _____
Professor Harold Y. Wachman
Chairman, Departmental Committee on Graduate Studies

Experimental Investigation of Contamination and Adhesion Failure of Type II Aircraft Ground De-Icing Fluids

by

Susanne Schroll

Submitted to the Department of Aeronautics and Astronautics on August 18, 1995 in partial fulfillment of the requirements for the Degree of Master of Science in Aeronautics and Astronautics

ABSTRACT

Federal aviation regulations state that an aircraft may not take off with frozen precipitation *adhering* to a flight surface. Commonly, the flight surfaces are treated with a thin layer of Type II de/anti-icing fluid to prevent aircraft ground de-icing. Few studies have addressed the issue of whether contamination of the fluid layer implies that the layer will not clear off during the ground roll.

There is therefore a need for a detailed study of the failure modes of Type II aircraft ground de-icing fluids exposed to natural precipitation conditions. The present study focused on determining if the fluid layer, contaminated by precipitation, adheres to the testing surface. The goal was to identify if a higher level of adhesion was associated with a particular failure mode. The approach was to experimentally measure the shear force required to clear naturally accumulated precipitation off a surface treated with Type II de-icing fluid. Four shear tests were carried out during two different snow events. Video recordings provided close up views of the contamination process and the shear process and allowed a rough estimate of the adhesion.

The limited amount of cases that were studied preclude a general conclusion. However, the observations did seem to indicate the existence of two distinct failure modes. The failure modes appeared to be related to the way the precipitation elements interacted with the fluid layer. A higher precipitation rate was observed to result in a bridging failure mode, where the contamination was separated from the test surface by a fluid layer. In this case the contamination progressed rapidly and abruptly, once the roughness became visible along the upper edge of the test plate. A lower precipitation rate led to penetration of the fluid layer, a three phased contamination process and generally higher adhesion. The research showed that adhesion failure does occur, is unambiguous and can be tested.

Thesis Supervisor: Robert John Hansman Jr.
Title: Professor of Aeronautics and Astronautics

Acknowledgments

This work was supported by the Federal Aviation Administration Grant # 93-G-019

The author would like to thank Octagon Process Inc. for supplying their product Octagon Forty Below De-icing/Anti-icing Fluid and ARCO Chemical Company for supplying Kilfrost ABC-3 Anti-icing Fluid.

Thanks also goes to Dr. James Riley of the Aviation Safety Division, Flight Safety Research Branch at the FAA Technical Center, Atlantic City International Airport, N.J. for providing comments on the research.

I thank my husband, Chris, for helping me with the experiments during the winter and for always being there for me.

Thanks also goes to my cousin, Annemette Schroll, who was able, on short notice, to leave Denmark to come and lend a helping hand during a very hectic summer.

This work is dedicated to my daughter, Natascha, who has had to put up with her mother's long hours of work during the last couple of years.

Table of Content

List of Figures

List of Tables

Chapter 4

Chapter 1

Introduction

1.1 Problem Statement

In 1950, the Civil Aeronautics Board (CAB) established regulations prohibiting the takeoff of an aircraft when snow, frost or ice is adhering to primary surfaces such as wings, ailerons etc. [FAA, 1982, AC 20-117]. These regulations still remain in effect and form the basis for the clean aircraft concept. It is known that aircraft performance and flight characteristics can degrade significantly when ice formations are present. Tests have indicated that roughness on the wings, similar to medium to coarse sandpaper, can decrease wing lift by as much as 30 percent and increase drag by 40 percent.

Specifically, the regulations say (FAR 91.527 Operating in Icing Conditions);

> *(a) No pilot may take off an airplane that has -*
>
> *(1) Frost, snow, or ice adhering to any propeller, windshield, or powerplant installation or to an airspeed, altimeter, rate of climb, or flight attitude instrument system;*
> *(2) Snow or ice adhering to the wings or stabilizing or control surfaces; or*
> *(3) Any frost adhering to the wings or stabilizing control surfaces, unless that frost has been polished to make it smooth.*

The key word here is *adhering*. Generally, as a practical rule, pilots do not takeoff when frozen precipitation is visible on any of the primary flight surfaces of the aircraft. Not much information is available about the level of shear required to remove the contamination layer. A detailed investigation of adhesion would provide a better understanding of the performance of de-icing fluids.

1.2 Research Objectives

Type II (Non-Newtonian) de-icing fluids were introduced in the US around 1985, with widespread use being common by 1990. These fluids are designed for use on aircraft with rotation speeds greater than 85 knots and are intended to provide protection in conditions conducive to aircraft icing on the ground [FAA, 1992, AC 120-58]. Commonly a heated solution consisting of water and Type I fluid is used to de-ice the aircraft followed by an application of un-diluted Type II fluid to anti-ice the aircraft before takeoff [Masters, 1991]. A large number of factors influence the degradation of the Type II fluid and thus the time of effectiveness of the fluid. As the fluid looses its ability to melt oncoming precipitation, a visible layer of frozen precipitation forms on top of the fluid layer.

There have been few studies addressing the issue of whether contamination of the fluid layer implies that the fluid-precipitation layer will not clear off during the ground roll (adhesion failure). There is therefore a need for a detailed study of the failure modes and mechanisms of Type II de-icing fluids. This research effort has been directed towards identifying the failure modes associated with adhesion.

The objective of the present research was to achieve a better understanding of contamination and adhesion of Type II de-icing fluids in order to help pilots develop workable procedures. The approach was to experimentally measure the shear force required to clear naturally accumulated precipitation off a surface treated with Type II de-icing fluid. Based on high magnification

recordings of the sliding process, a description of the observed mechanisms leading to failure is provided.

The large number of variables present in the problem necessitates keeping many of them constant in order to obtain useful and comparable data. It was for that specific reason that Type II fluid was used in the un-diluted condition. Furthermore, all test plates in the study were kept at the same 10 degree inclination angle and only flat test surfaces were used. The important variables in the problem were;

- outside air temperature (OAT)
- precipitation type
- precipitation size
- liquid equivalent precipitation rate

1.3 Thesis Outline

This report documents the experimental work carried out during winter 1994/1995. Four experiments were conducted during February of 1995 in conditions of light snow, heavier snow and freezing rain. Chapter 2 provides an account of what motivated the present research and an introduction to Type II de-icing fluids. The test setup plus test and analysis procedure are described in Chapter 3 with the results in Chapter 4. Chapter 4 includes a description of a typical sliding process. The contamination and shear process are described for each of the four test cases based on the observations. Chapter 5 identifies and describes two distinct failure modes observed to influence adhesion. Chapter 6 contains a brief summary of the findings and a recommendation for further work.

Chapter 2

Motivation and Background

This chapter provides an overview of the issues that have motivated the present research project. A summary of other, on-going or recent, related research is presented along with a short introduction to de-icing fluids, in particular Type II fluids.

2.1 Motivation

Lack of de-icing or improper ground de-icing/anti-icing has been a contributing factor to at least 13 large transport aircraft accidents in North America since 1968 [Haase, 1991]. Of these 13 accidents, four involved aircraft that had been de-iced. The pilot in command is responsible for ascertaining that the aircraft adheres to the clean aircraft concept before proceeding for takeoff. This might be done by a visual inspection of the primary surfaces by doing a "walk around" or by shining light on the surfaces from the cockpit or the cabin. In general, a repetition of the de-icing process will be requested if precipitation is visible on the surface of the de-icing fluid.

In the accidents that involved aircraft that had been de-iced, there was a recognition on part of the pilot in command that the weather conditions were severe enough to warrant going through de/anti-ice procedures. The immediate safety issue then becomes the ability of the crew to judge the level of degradation of the de-icing fluid at a given time and when to request de/anti-

icing again. The microphysical aspects of fluid degradation have been documented by the extensive experimental research done by Anagnostakis [1994]. The research involved observing, through the use of a high magnification camera, the impact and melting of natural precipitation on surfaces treated with Type II de-icing fluids. More than 50 cases, each with a different set of environmental conditions and test surface geometry, were recorded. The outcome of the research was a classification of the stages of fluid degradation into an initial, an intermediate and a final stage.

The research done during the past year has been motivated by the results of the work carried out by Anagnostakis. The extent of degradation of the de-icing fluid is best determined by a visual inspection. However, visible precipitation on top of the fluid layer does not necessarily imply that the aircraft will not be in compliance with applicable FAR regulations. The next logical step, after classifying the stages of contamination, was to test if the fluid-precipitation mixture adheres to the testing surface. This was done by measuring the force required to clear the surface. The idea is to identify the failure modes associated with adhesion.

Before the uniqueness of the issues associated with Type II fluids can be appreciated, an understanding of the basic differences between Type I and Type II de-icing fluids is required.

2.2 De-Icing Fluids

The most common techniques for ground de-icing/anti-icing of aircraft employ Freezing Point Depressant (FPD) fluids. Commonly, the de/anti-icing process consists of two steps. First the aircraft is de-iced using a mixture of heated water and Type I or Type II de-icing fluid. Next, a thin protective layer of Type II fluid is applied to delay reformation of snow, ice or frost [Masters, 1991]. The de-icing fluids depress the freezing point of the resulting mixture which is characterized by its ability to melt the incoming precipitation. As the buffer between the freezing point of the mixture and the OAT becomes smaller due to addition of water in the form of snow, ice or freezing rain, the effectiveness of the fluid decreases.

Two types of de-icing fluids are available. Both types of fluids are glycol based solutions. Figure 2.1 shows a typical phase diagram for aqueous glycol solutions.

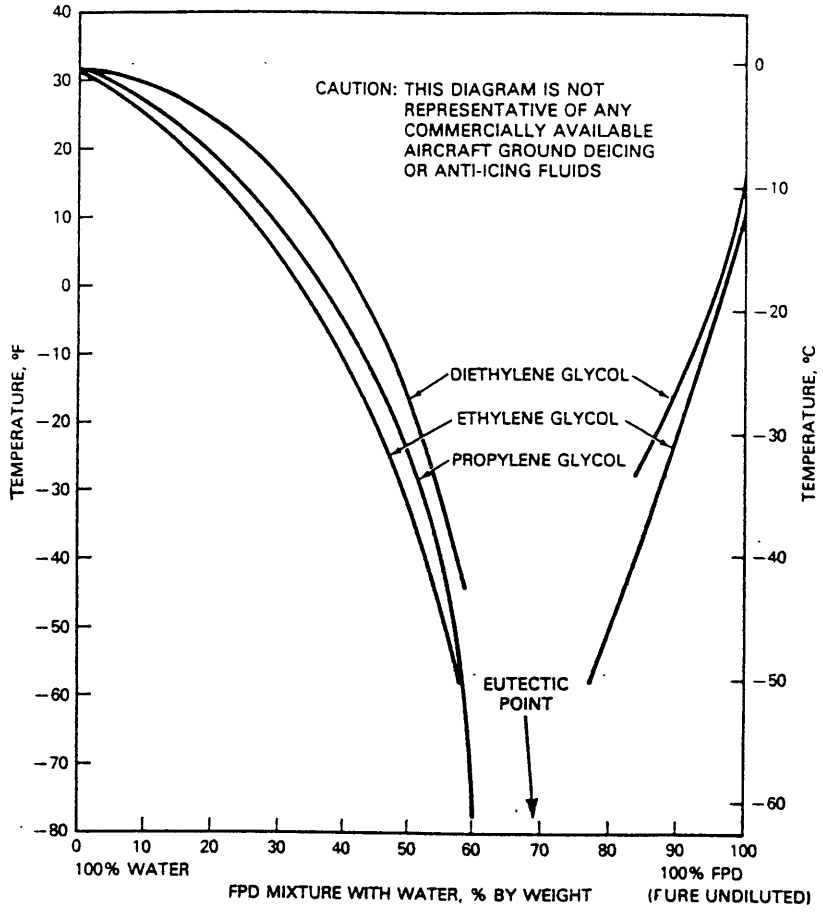

Figure 2.1: Phase diagram for Aqueous Glycol Solutions [AC 20-117]

Type I fluids exhibit Newtonian characteristics i.e. a linear relationship between shear stress and shear strain for any non-zero shear stress and therefore a constant apparent viscosity. These fluids have relatively low viscosity and are considered "unthickened". Their usefulness in providing anti-icing protection is therefore very limited.

Type II fluids have thickening agents added to enable the fluid to remain on the aircraft surfaces during standstill. Type II fluids have Non-Newtonian characteristics and are termed pseudoplastic. These substances require a finite stress to be applied before shearing occurs. This property makes the fluid ideal for the anti-ice application since it facilitates the application of a thicker

protective film. There is, however, a trade-off between the thickness of the fluid and its ability to flow off during the ground roll. The viscosity of the fluid is also temperature dependent, with a general trend of lower viscosity at lower temperatures [Ross, 1991].

Chapter 3

Test Setup and Procedure

One of the objectives for the research was to experimentally measure the shear force required to clean a surface with real precipitation. A test facility consisting of an exposure rig and a shear test rig was built for that purpose. A test procedure for determining the required shear force was developed. Fluid was furnished for the study by ARCO Chemical Company (Kilfrost ABC-3 fluid) and by Octagon Process Inc. (Octagon Forty Below). In each of the four cases studied an equal number of test plates were treated with each fluid and shear testing of the two fluids were done simultaneously as explained in the test procedure section. A difference in viscosity was apparent when pouring the fluids. The Octagon fluid would spread over the plate sooner than the Kilfrost plate.

3.1 Test Setup

Figure 3.1 below shows the exposure rig. The exposure rig was designed to hold a series of test plates at an angle of 10 degrees. The 3" x 3" polished aluminum test plates were hooked on the strip and exposed to precipitation at an inclination angle of 10 degrees. The hook on the plates made it easy to remove a plate without disturbing the accumulated precipitation. Half of the test plates on the exposure rig were treated with Kilfrost fluid, the other half with Octagon fluid. The control plate was not treated with any fluid, but inclined at the common plate angle and exposed to precipitation.

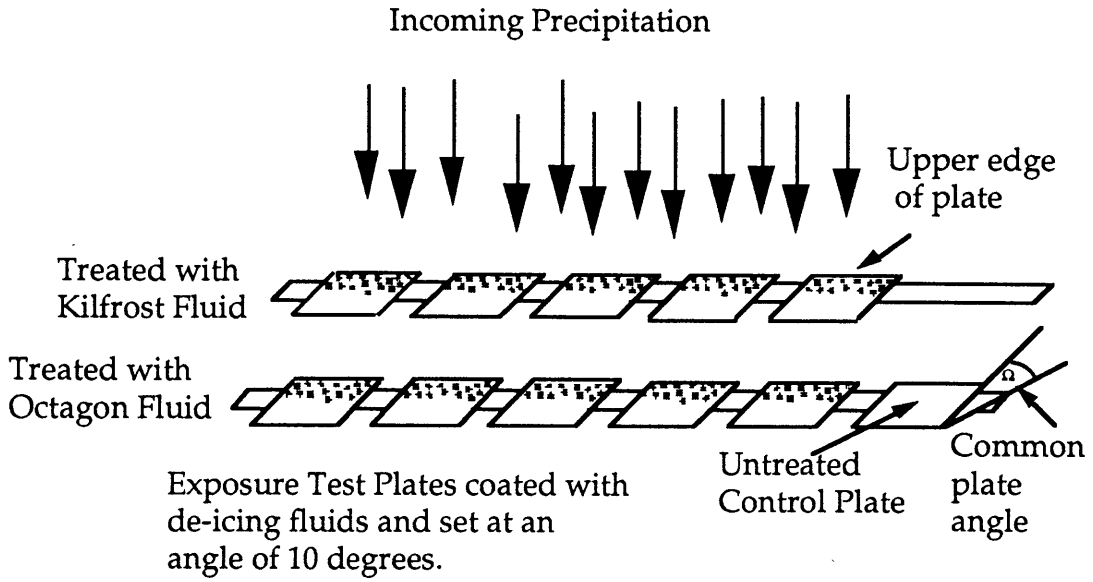

Figure 3.1: Exposure Rig

The shear test rig was located in a sheltered area at the same temperature as the exposure area temperature. Figure 3.2 shows a schematic of the shear test rig. The shear test rig consisted of a rectangular plate mounted on top of a rotary motor. A fixture at each end of the plate allowed a test plate and a fluid collection container plus tube to be attached. The length of the spin arm was 19 cm to the inner edge of the test plate. The motor allowed the test plate assembly to be spun at a rotational speed of up to 350 rpm corresponding to a velocity of 7 m/s at the inner edge of the plate.

The fluid collection container was made from clear plastic which made it possible to record a magnified image of the behavior of the precipitation/fluid layer. A strobe light, triggered by a light pick-up, provided a frozen image of each plate and the frequency counter once per revolution. The camera was positioned about 3 ft from, and approximately normal to the test plate surface, to reduce glare. The camera viewed the entire surface of the test plate and a portion of the arm that identified which fluid mix was in view. The fluid collection tube was detachable and used for collecting the contamination sheared off during the shear test.

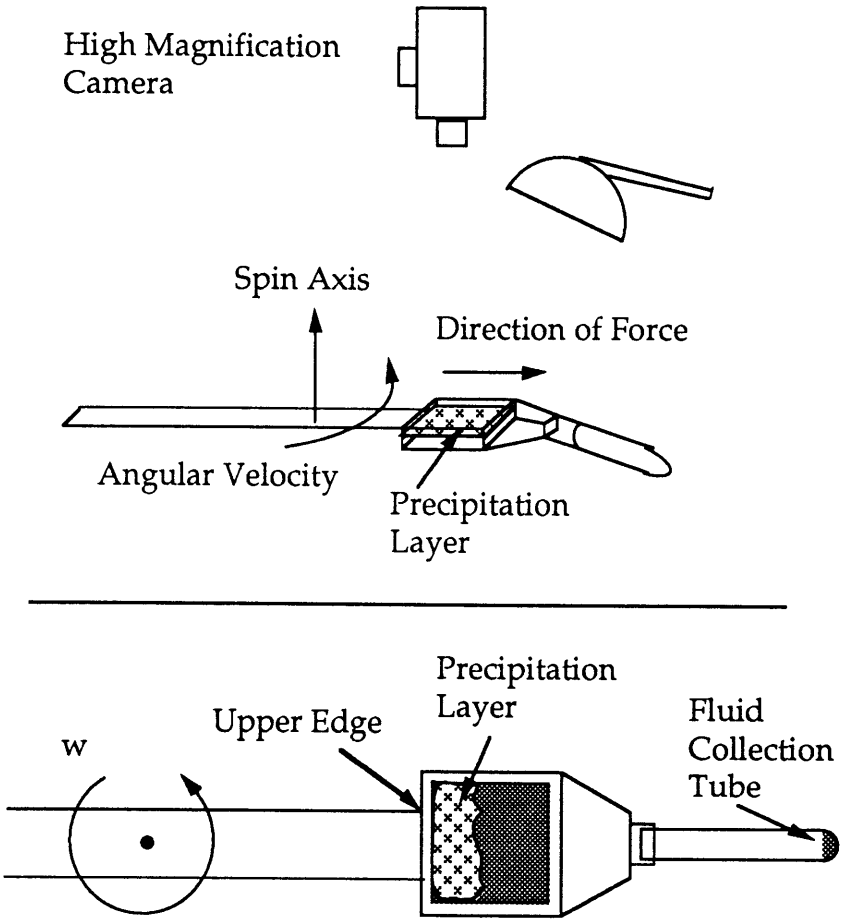

Figure 3.2: Shear Test Rig.

Two reference plates, separate from the exposure test plates, were used for recording high magnification video images of the precipitation impact throughout each experiment. The setup is shown in figure 3.3. The camera, located indoors, viewed the two 3"x 3" fluid covered reference plates through a window. Each plate was covered with a different brand of de-icing fluid and set at an angle of 10 degrees. A grid plate contained in the view area aided in estimating the flake size and allowed a comparison between the contamination coverage of a treated and an untreated plate. The distance between camera and test plates was approximately 5 ft. This distance was too large to allow for a very detailed view, but adequate to document the amount of precipitation coverage versus time.

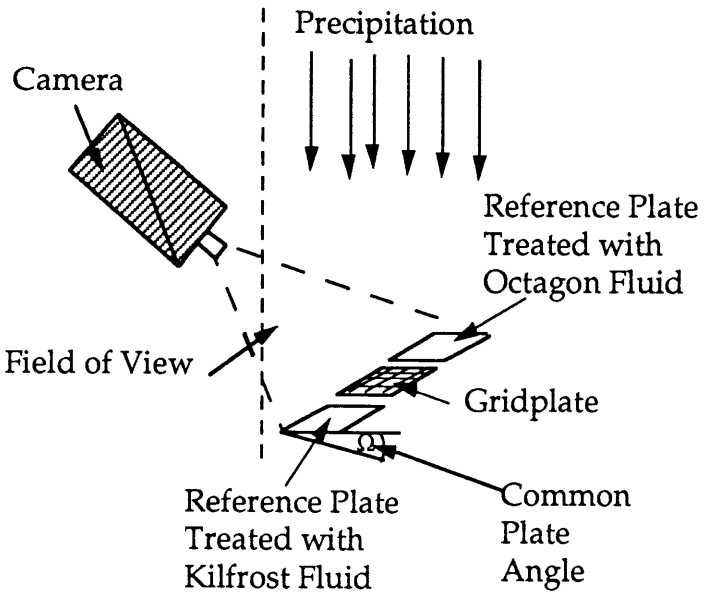

Figure 3.3 Setup for Recording of Reference Plates

3.2 Test Procedure

The test setup was on standby and readied whenever the weather forecast indicated a snow event was approaching the Boston area. Preparing for the test consisted of setting up for the high magnification static recording, readying the exposure rig and testing the shear test rig.

3.2.1 Recording of Reference Plates

The 3" x 3" aluminum reference plates were placed outside, together with the grid plate, well before the precipitation event begun to ensure that the plate surfaces were at ambient temperature. The camera position and light were adjusted to a obtain a clear, focused view of the test area. When the precipitation begun the two surfaces were cleaned of any accumulated snow or ice and an amount, sufficient to quickly cover the area, of fluid was poured at the upper edge of each surface. One surface was covered with "Octagon Forty Below" manufactured by Octagon Process Inc. [Octagon Product Documentation] the other with "Kilfrost ABC-3" manufactured by ARCO Chemical Company [Kilfrost Product Documentation]. Both fluids were applied undiluted (neat), at room temperature using a beaker. As soon as the reference plates were covered with fluid the recording started. Outside temperature, precipitation type, date and time were noted. The recording was left to run until the shear test had finished.

3.2.2 Exposure of Test Plates

The exposure rig was placed outside in an area sheltered from the wind, but with an unobstructed path for the precipitation. The test plates were kept at ambient (outside) temperature in a sheltered area until the experiment was ready to start. At the start of the experiment the plates were hooked onto the exposure rig. Any film buildup or dirt was removed before treating the test plates with de-icing fluid. An equal number of test plates were covered with Octagon fluid and Kilfrost fluid. The control plate was left untreated. The

fluid, undiluted (neat) and at room temperature, was poured at the upper edge of each plate. As soon as the fluids were poured the time, temperature and precipitation type etc. were noted. A pan, for measuring the liquid equivalent precipitation rate was placed near the exposure rig at an angle of 10 degrees. A snow gauge, consisting of a plate with a vertically mounted ruler, was placed outside. The start time of exposure was noted for both gauges.

3.2.3 Shear Test

The shear test rig was readied to make sure that the camera position and the strobe lighting would result in an clear, focused image with minimal glare. A heating pad on the motor was turned on to prevent the motor from displaying start up variations in speed due to cold lubrication. When visible precipitation started to accumulate on any of the test plates a set of plates (one with Octagon, one with Kilfrost), together with a fluid collection container and tube, were attached to the rotor arm. The plates were oriented with the upper edge closest to the center of rotor arm. The orientation was chosen to avoid addition of fluid into the sliding process. Addition of fluid into the sliding process would have caused a further mixture of de-icing fluid and contamination and thus the sliding process would not represent the process associated with the estimated contamination coverage.

A static image of each plate was recorded before the spinning started. The speed of the motor was varied in steps of 50 rpm, at 30 second intervals, starting from 100 rpm up to 350 rpm. This allowed new sets of plates to be spun frequently enough to furnish useful data. The threshold acceleration was determined from the speed at which precipitation at about a quarter of an inch from the upper edge started to move. The light meter on the high magnification recorder was adjusted so that only the strobed image of each plate and the LED display on the frequency counter were visible on the VCR recording.

The camera recorded an image of the behavior of the precipitation-fluid layer on each plate once per revolution during spinning. At the end of the sequence a static image was recorded again and the plates were removed. A

clean surface was defined to be a surface that was free of residue other than isolated spots the size of a few grains of sand. Edge effects along upper and side edges were ignored. The fluid collection container and the tube was left in a horizontal position to allow any fluid remaining in the container to run down in the tube. The sequence was repeated at fixed time intervals whose length depended on the precipitation rate.

The runs continued until the treated plates were completely covered by precipitation. After the last run the control plate was mounted and spun in order to provide a basis for determining the benefit from de-icing fluid treatment.

The temperature was recorded at least twice during the experiment. After the shear test was finished the depth of snow was measured and the snow collected in the pan was melted and weighed in order to determine the liquid equivalent precipitation rate. The precipitation-fluid mixtures collected in the tubes were saved for later analysis.

3.3 Data Analysis Procedure

3.3.1 Contamination Analysis

Many definitions of what constitutes a contaminated fluid layer exist. Because of this, a set of conventions were used in analyzing the collected data. Areas of contamination were estimated based on the classification of contamination developed by Anagnostakis [Anagnostakis]. Three stages of contamination were recognized. These were;

- **Initial stage**
  During this stage the fluid is able to completely melt the incoming precipitation and no visible precipitation accumulation occurs.

- **Intermediate Stage**
  This stage is characterized by the *inability* of the fluid to fully

melt incoming precipitation elements. The time to melt an incoming element increases as the fluid becomes degraded and the fluid film enters the slush stage. The incomplete melting results in the accumulation of a precipitation layer on the fluid surface.

- **Final Stage**

  In this stage additional layers of precipitation (snow bridges) form on top of the initial layer. The elements in these layers do not melt at all and fail to disappear in the film.

The estimation of contamination coverage at a given time was based on the percentage of the total surface area covered by intermediate or final stage contamination. In general contamination would start along the upper edge and proceed down the plate as the exposure time increased. The coverage was estimated from the VCR recording of the exposure test plate before it was spun. Areas of contamination were evidenced by surface roughness for late intermediate and final stage contamination and by a loss of gloss on the fluid surface for early intermediate stage. In the description of adhesion % line refers to a line across the plate, parallel to the upper edge of the plate, at the indicated distance, i.e. 25% line refers to a line a quarter down the plate from the upper edge.

3.3.2 Shear Analysis Method

A shear analysis method was developed in order to calculate the shear stress. Based on the images of the contamination layer during the shear test, the threshold acceleration, at which contamination near the upper edge started to move down the plate, was obtained. The sheared off contamination (mixture of fluid and precipitation) was collected in the tube and later weighed. A method was necessary in order to infer the shear stress from the acceleration data.

Figure 3.4 shows a schematic of the contamination layer used for the shear analysis. The schematic does not represent an exact picture of the layer, but is does allow a rough estimate of the shear to be calculated. The schematic is

based on the following approximations;

- uniform layers of precipitation and fluid
- shear element slides as a block at the observed rotational speed
- precipitation mass = total mass - estimated fluid mass

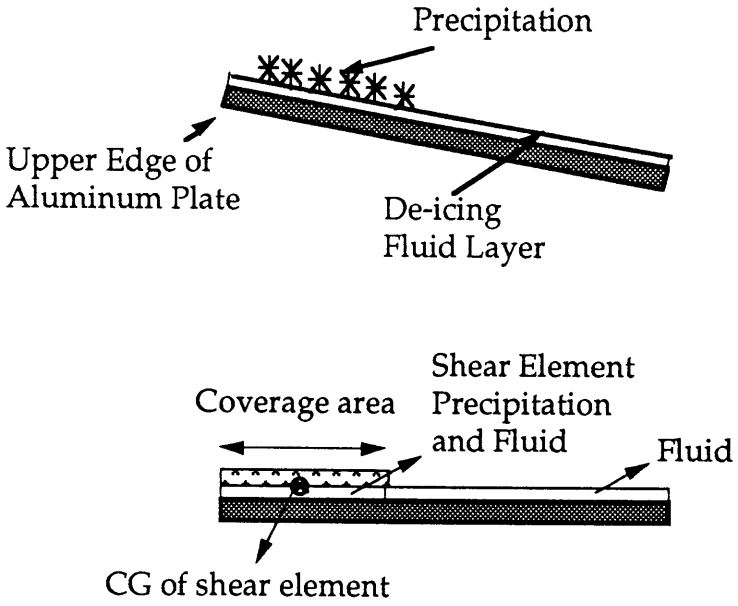

Figure 3.4: Theoretical Shear Model.

The procedure for calculating the shear was as follows;

1) Estimate visible precipitation coverage (in terms of percentage of total surface area covered by intermediate or final stage contamination).

2) Determine rotational speed (corresponding to threshold acceleration) at which sliding starts at 1/4" from the upper edge of the plate by comparing *before* spin picture with *during* spin picture (obtained from VCR recordings).

3) Calculate shear at sliding based on coverage area and shear element mass and observed threshold acceleration.

The total mass was obtained by weighing the fluid/precipitation mixture collected during the shear experiment. The shear element mass was calculated as the difference between total mass and fluid mass. The estimated fluid mass was based on runoff data for each brand of fluid. Runoff data were obtained by placing a number of plates covered with Octagon or Kilfrost fluid outside in (1°C) non-precipitation conditions. At five minute intervals a set of plates were mounted on the rotary arm and spun. The sheared off fluids were collected in a tubes. Each tube was weighed to determine the fluid mass. Figure 3.5 shows the remaining mass of fluid versus time interval for the two fluids.

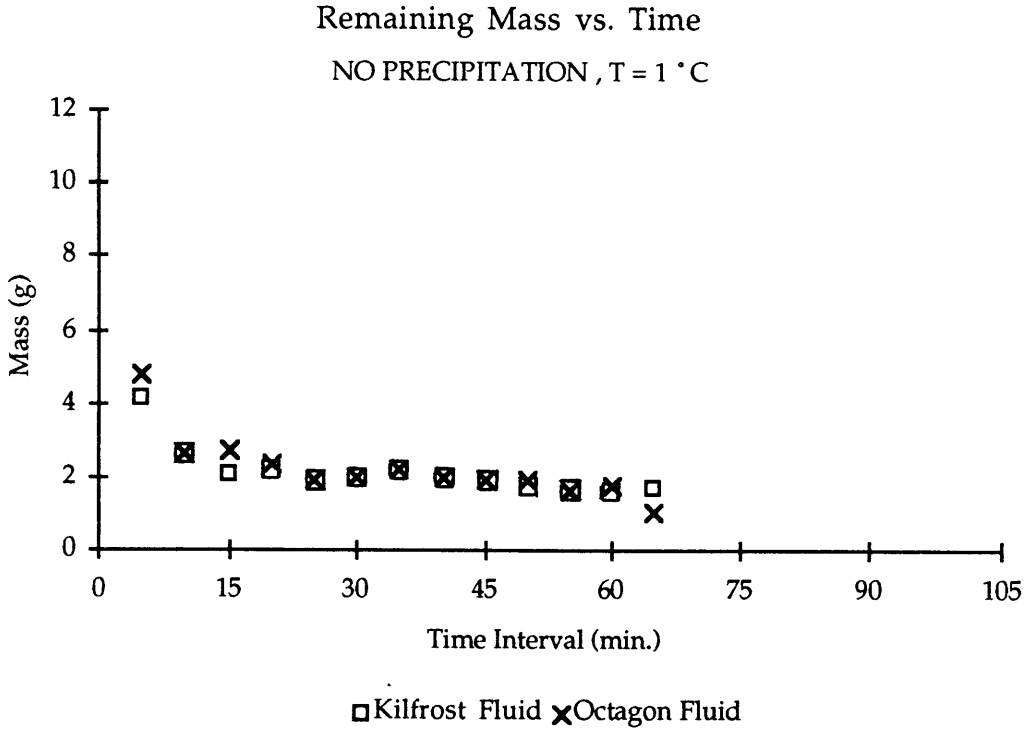

Figure 3.5: Remaining Mass versus Time (Runoff Data).

The data for each fluid was curve fit to allow an estimation of remaining fluid mass on the test plate at a given time. Appendix A contains curve fit data for Octagon and Kilfrost fluid. The runoff of the fluids are seen to follow an exponential curve with decreasing runoff with time. It was assumed that fluid runoff was independent of precipitation rate and temperature. Actual runoff during precipitation may be different and this constitutes a potential error source.

Chapter 4

Field Data

Four shear tests were carried out during two different snow events in February 1995. This chapter provides a summary of the data, a description of a typical sliding process and a description of the contamination and adhesion observed in each of the four tests. The description of the contamination process is based on the observations of the reference plates and on the percent coverage estimated from the images of the test plates. In each case the trend on the reference plates and the test plates was the same. However, the recording of the reference plates provided a view of the entire contamination process whereas the images of the test plates were taken at given time intervals. The recorded images of the sliding process on the test plates provided insight into the mechanisms behind adhesion.

4.1 Summary of Data

Table 4.1 shows a summary of the data obtained during the four tests. LEPR refers to *liquid equivalent precipitation rate* and was determined by melting the precipitation collected in the pan, and weighing the amount of water. The snow depth was read off the snow gauge and the snow rate (mm/hr) was determined. The density was calculated from the snow depth (m), the area of the pan (m^2) and the mass (kg) of the melted snow.

Table 4.1: Data Summary for De-icing Fluid Experiment.

Date	Case #	Temp (°C)	PRECIPITATION			
			Type	Rate (mm/hr)	LEPR ($g/dm^2/hr$)	Density (kg/m^3)
2/4/95	1	- 2	Light snow small flakes	11.7	13.7	117
2/4/95	2	- 1	Heavier snow medium flakes	30.5	38.9	128
2/27/95	3	-6.8 to -8.3	Light snow very small flakes	12.7	6.0	48
2/27/95	4	-1.5 to -6.7	Light freezing rain	2.4	5.9	243

4.2 Typical Sliding Process

Test plates treated with fluid went through a typical sliding process if sufficient shear was induced through spinning. The test plates were inclined at an angle of 10 degrees during exposure in order to emulate standard frosticator plate tests. In this position contamination was observed to start at the upper edge and proceed down the plate as the exposure time increased. The sliding process consisted of three, more or less distinct, phases as shown in the figure 4.1;

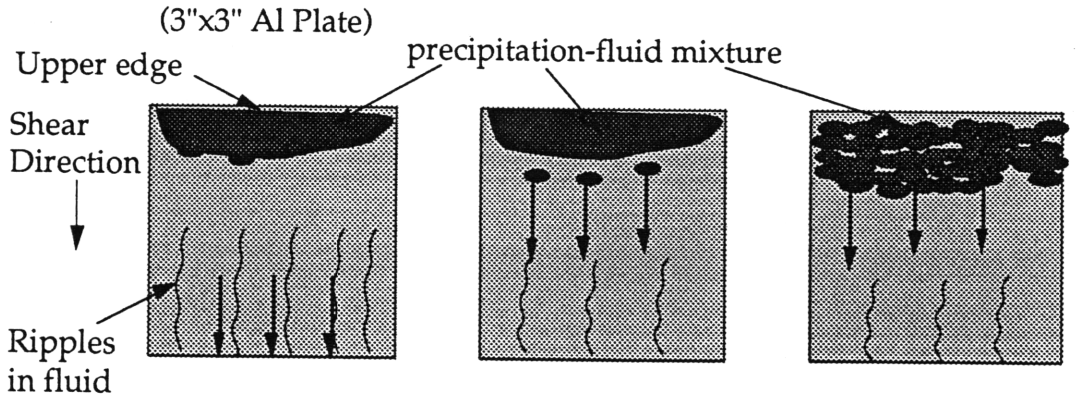

Figure 4.1: Typical Sliding Process

At low acceleration ripples were observed in the fluid-only (i.e. no visible precipitation) layer, starting at the bottom edge of the plate where the acceleration is higher. The fluid started flowing off , but no movement was yet observed of the precipitation-fluid mixture layer. As the acceleration was increased the lower part of the precipitation-fluid mixture layer started to break up and flowed off the plate.

At the threshold acceleration precipitation-fluid mixture near the upper edge broke up and started moving down. An example of this is shown in figure 4.2.

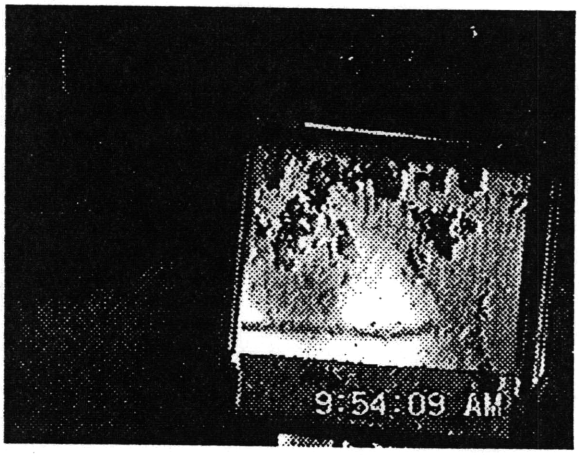

Figure 4.2: Example of Precipitation-Fluid Mixture Sliding off the Test Surface in Discrete Lumps.

The acceleration at which the precipitation-fluid mixture broke up was defined as the threshold acceleration. In the case of test plates fully covered with precipitation-fluid mixture (longer exposure time) ripples were not observed and sliding did not start until the precipitation-fluid mixture layer broke up.

Test plates not coated with de-icing fluid showed a slightly different sliding behavior. In the cases where the precipitation did not adhere to the test surface the entire precipitation layer was observed to slide off together in one big lump. An example of this is shown in figure 4.3, taken while spinning the untreated plate in Case 1.

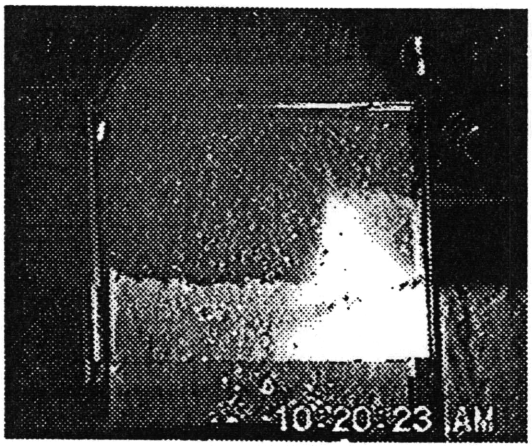

Figure 4.3 : Example of the Entire Snow Layer Sliding off a Control Plate

4.3 Case 1: Light Snow, Small Flakes

4.3.1 General Description

Test 1 was carried out during a snow event in the Boston area on February 4, 1995. The two fluids were applied undiluted, at 8:47 am, to test plates tilted at an angle of 10 degrees to the horizontal. The recorded temperature of -2°C, at 8:45, remained constant throughout the experiment. Visible snow accumulation was observed on the test plates 35 minutes after fluid application. The precipitation consisted of small, wet snow flakes with a snowfall rate of 0.46" per hour as recorded by the snow gauge. The average snow density was 117 kg/m^3 based on a time period of 1.5 hours. The average liquid equivalent precipitation rate (LEPR) was 13.7 $g/dm^2/hr$. The snowfall rate increased slightly towards the end of the exposure.

4.3.2 Case 1: Contamination

A graphical representation of the observations of the images of the test plates illustrates the general contamination process. Figure 4.4 shows the percentage of each plate covered by intermediate or final stage contamination

versus the plate exposure time.

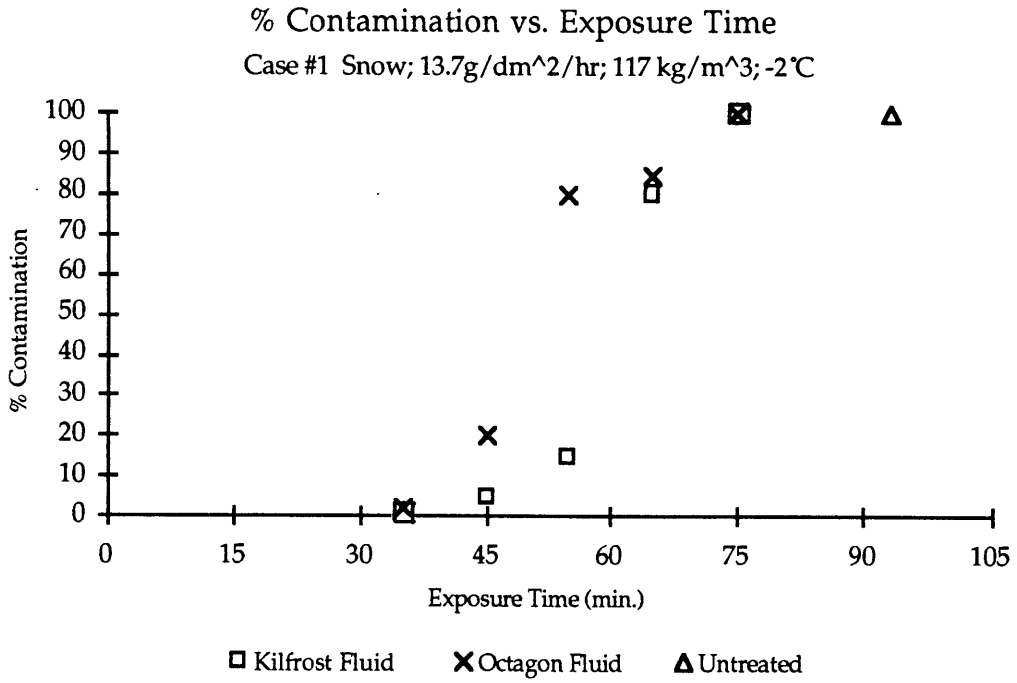

Figure 4.4 : Case #1: % Contamination versus Exposure Time

The contamination process for both fluids was similar except that the process for Kilfrost fluid was delayed as shown in figure 4.4. After a given time the melting time of the snow flakes appeared to increase and slight build-up along the upper edge became visible. The area of contamination increased in a direction down the plate along a fairly regular line across plate. Initially the rate was relatively slow as evidenced by the plotted data in figure 4.4. After the area close to the upper edge of the plate was contaminated, the rate increased significantly and the majority of the plate became covered in a short time. When the contaminated area approached the bottom edge of the plate the rate decreased again until the plate was fully covered.

This three phase effect could be explained in terms of the fluid layer profile. Along the upper edge the layer is thinnest and will tend to get depleted as precipitation impacts the surface and runs off. The middle part of the plate has a thicker layer and thus an ability to melt incoming precipitation ele-

ments for a longer time. Meniscus effects are present along the bottom edge of the plate and result in a relatively thicker fluid layer which explains why the rate of contamination decreases close to this edge. Of the three phases, the first and the third can thus be attributed to edge effects leaving the second phase as the important one. The plotted data show that contamination of the majority of the plate occurs very sudden.

Figure 4.4 show that the contamination of the Kilfrost fluid was delayed compared to the Octagon fluid. The onset of the second phase occurred later for the Kilfrost fluid, but the fluid appeared to catch up with the Octagon fluid and both plates reached the same high level of contamination at approximately the same time. Figure 4.5 shows the difference between the two fluids after an exposure time of 55 minutes.

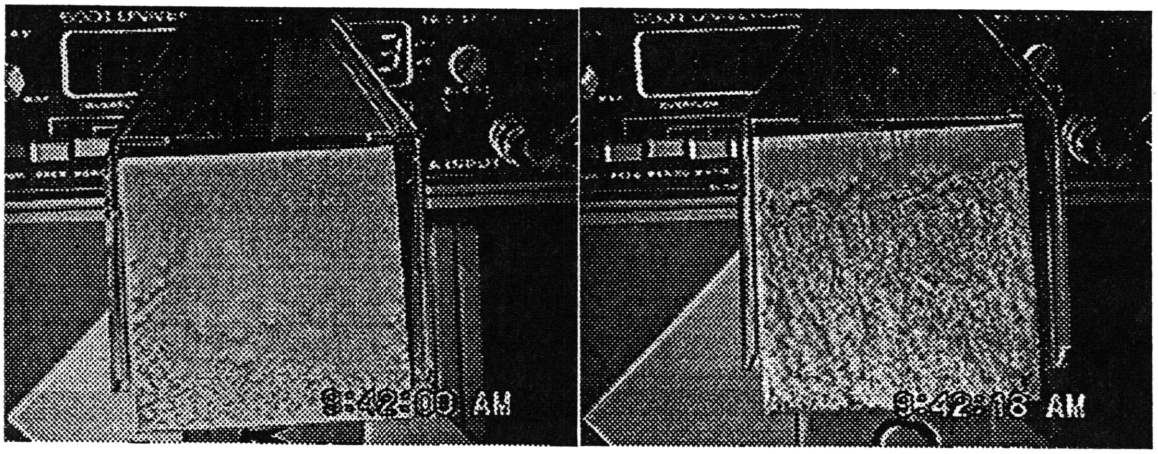

Figure 4.5a: Case 1; Kilfrost Exposure plate at 55 minutes

Figure 4.5b: Case 1; Octagon Exposure plate at 55 minutes

Figure 4.6 below shows the mass that was collected in the fluid collection tube during spinning for Test 1. The collected mass was seen to initially decrease. This is thought to be due to the fluid running off faster than the precipitation accumulates. Both fluids followed the same trend and similar masses were collected for each fluid. The mass collected at 93 minutes was from the untreated control plate and consisted of precipitation only. As the exposure time increased a larger percentage of the collected mass consisted of melted or frozen precipitation. The 45 minute point represented minimum mass for both fluids. Any addition in mass past this point was due to accu-

mulation of precipitation only.

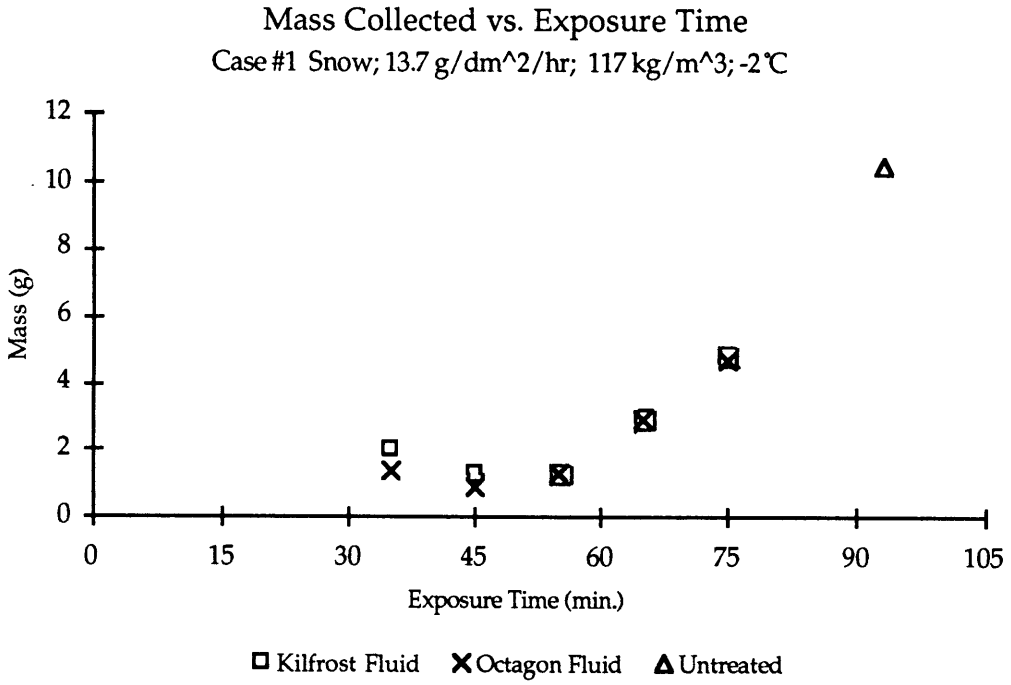

Figure 4.6: Case #1: Mass Collected versus Exposure Time

4.3.3 Case 1: Adhesion

The high magnification recording of the test plates during the shear test provided insight into the sliding process of the fluid and the precipitation-fluid mixture layer. The first set of plates were spun 35 minutes after applying the fluids. After that another four sets of plates were spun at 10 minute intervals. At the end of the sequence the untreated control plate was spun.

The first set of plates had almost no visible contamination. At a speed of 200 rpm ripples were observed in the direction of the force on both plates. The fluids were observed to initially pile up near the bottom edge of the test plates and then flow off.

Ten minutes later contamination on the Kilfrost plate remained light

while about 20% of the area on the Octagon plate was contaminated. The slight contamination on the K plate started to move down the plate at a speed of about 250 rpm. Again ripples were observed in the fluid layer below the contamination at a lower speed. The plate was completely clear afterwards. The contamination layer near the upper edge on the O plate started to break-up and move down at a speed of 250 rpm. The contamination on the Octagon plate flowed off in discrete lumps along the ripples in the fluid.

At an exposure time of 55 minutes contamination on the Octagon plate had reached 80% while the Kilfrost plate only had 15% contamination. It was difficult to see the sliding process on the Kilfrost plate, but is appeared that contamination was flowing off at about 150 rpm. At a speed of 200 rpm the plate was observed to be clear. Ripples were visible in the fluid layer near the lower edge of the Octagon plate at 150 rpm and precipitation along the lower edge had started flowing off. At 250 rpm the contamination layer had thinned and moved away from the upper edge. The contamination was observed to move down the plate in streams.

Both test plates at an exposure time of 65 minutes had the same high level (approximately 80%) of contamination. Ripples were visible in the fluid layer close to the bottom edge of the Kilfrost plate at a speed slightly below 200 rpm. As the speed approached 250 rpm most of the contaminated layer had broken up into big lumps and started flowing off. The lumps looked wet and generally moved down in a smooth manner. The Kilfrost test plate was completely clear afterwards. The contamination on the Octagon plate started breaking up along the lower edge at around 200 rpm. At 250 rpm the upper edge of the contamination layer was observed to move down the plate in small lumps along the streamlines of the fluid. Some small residue was left on the right side and in a line across the middle of the plate.

The untreated control plate had a thick layer of snow. The snow was observed to move down around a speed of 100 rpm. The snow layer did not break up but slid off as a solid mass.

Figure 4.8 below shows the shear stress required to clear the test plate surface of contamination.

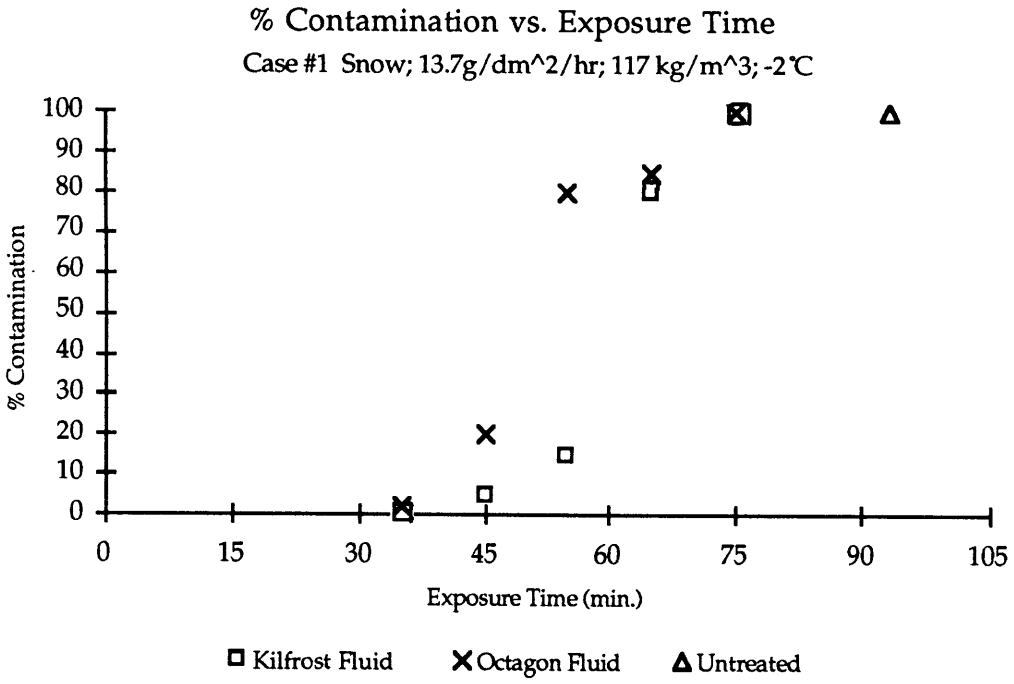

Figure 4.7 : Case #1: % Contamination versus Exposure Time

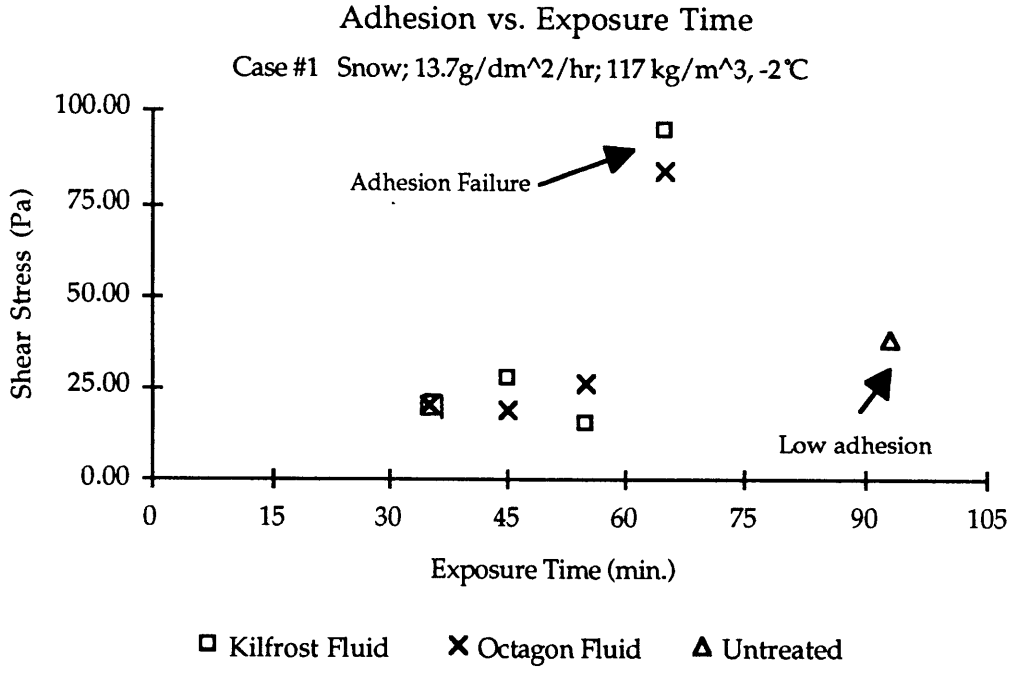

Figure 4.8: Case #1: Adhesion versus Exposure Time

The data points for figure 4.8 were obtained using the shear analysis method described in chapter 3. The graph of % Contamination versus Exposure Time has been included (figure 4.7) to provide a basis for comparing level of contamination with adhesion. Past 55 minutes a large increase in adhesion was observed, which indicates that adhesion failure has occurred.

A comparison of the data in figure 4.7 and 4.8 showed that more than 80 percent of the area of the test plate was contaminated before adhesion failure occurred. For both fluids, adhesion failure occurs before full coverage. The adhesion for the untreated control plate was above the failure limit, but below the adhesion at full coverage on the treated test plates. The adhesion for Octagon increased significantly between 55 and 65 minutes, however no significant increase in % contamination occurred. Although the coverage did not increase much there was an increase in collected mass which resulted in a higher shear level.

4.4 Case 2: Heavier Snow, Medium Flakes

4.4.1 General Description

For Case 2 the plates were treated with undiluted (neat) Octagon and Kilfrost fluid at 11:36 am during the same snow event as Case 1. The average size of the snow flakes had increased to medium, compared to Case 1, and the average rate increased to 1.2" per hour. The density of the snow increased, compared to Case 1, to 128 kg/m^3, while the LEPR almost tripled to 38.9 $g/dm^2/hr$. The temperature was measured to be -1°C at 11:40 am and remained constant throughout the experiment. No significant change in snowfall rate was observed during the experiment, however, light gusts of wind were present in the exposure area. Visible snow accumulation was observed after an exposure time of 10 minutes.

4.4.2 Contamination

Figure 4.9 shows the % contamination of the plates as estimated from the images of the test plates. The precipitation rate in this case (Case 2) was thrice

that of Case 1. A comparison of the two cases show that the time at which contamination first became visible decreased by approximately a third in Case 2. In Case 1 the contamination process appeared to consist of three phases. In Case 2 with a higher precipitation rate only two phases were evident. Contamination was observed to occur at a high rate until the majority of area of the test plates were contaminated. Again the slower rate of accumulation near the bottom edge can be attributed to the effect of meniscus. The time it took for the majority of the area of the plate to become contaminated was similar for Case 1 and 2.

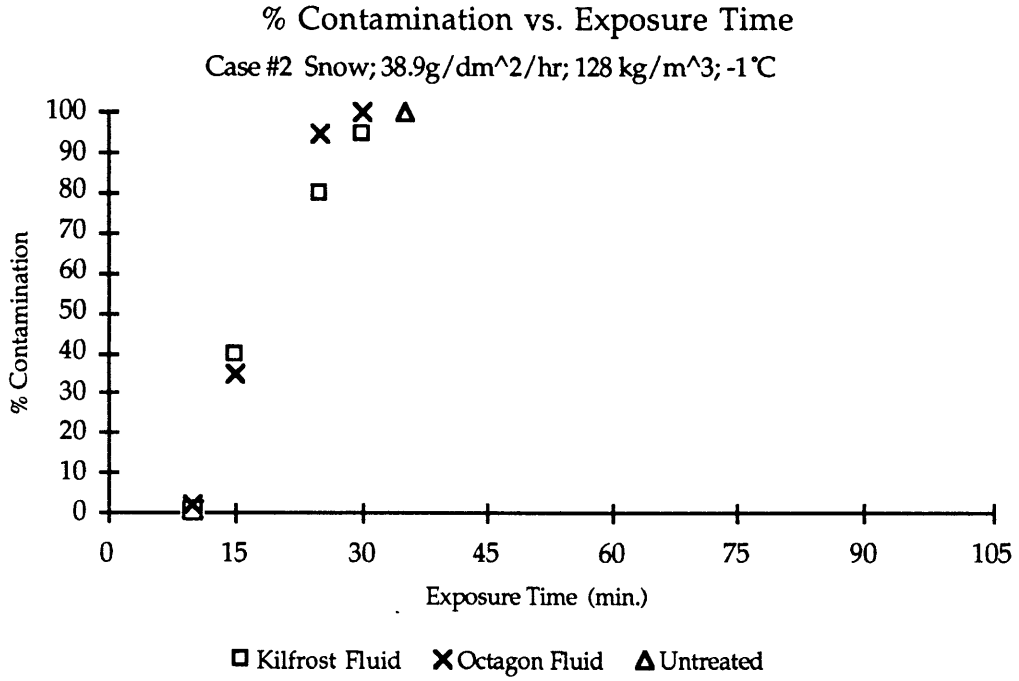

Figure 4.9: Case #2: % Contamination versus Exposure Time

There appeared to be no significant difference in the contamination process of the Kilfrost and the Octagon fluid in this case. Figure 4.10 is a view of the exposure plates after an exposure time of 15 minutes.

The contamination occurred very rapidly and did not proceed down the plate along a regular line. The high rate of contamination might have obscured any differences in fluid behavior, but for all practical purposes the deg-

radation of the two fluids was similar.

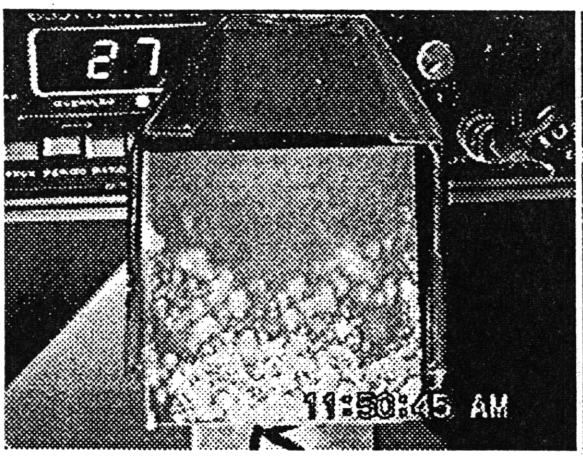

Figure 4.10a: Case 2; Kilfrost Exposure plate at 15 minutes

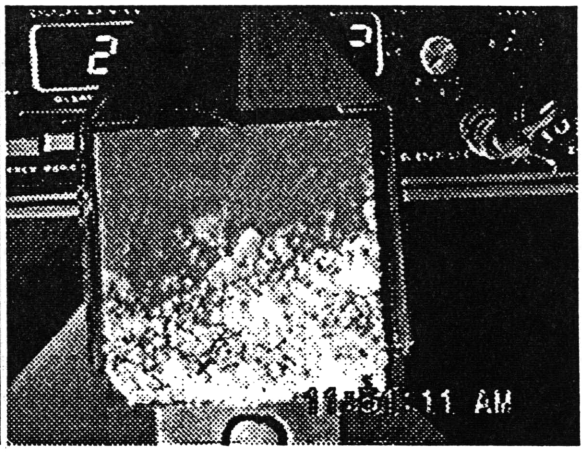

Figure 4.10b: Case 2; Octagon Exposure plate at 15 minutes

Figure 4.11 below shows the masses that were collected in the tube at each time interval during the shear test in Case 2.

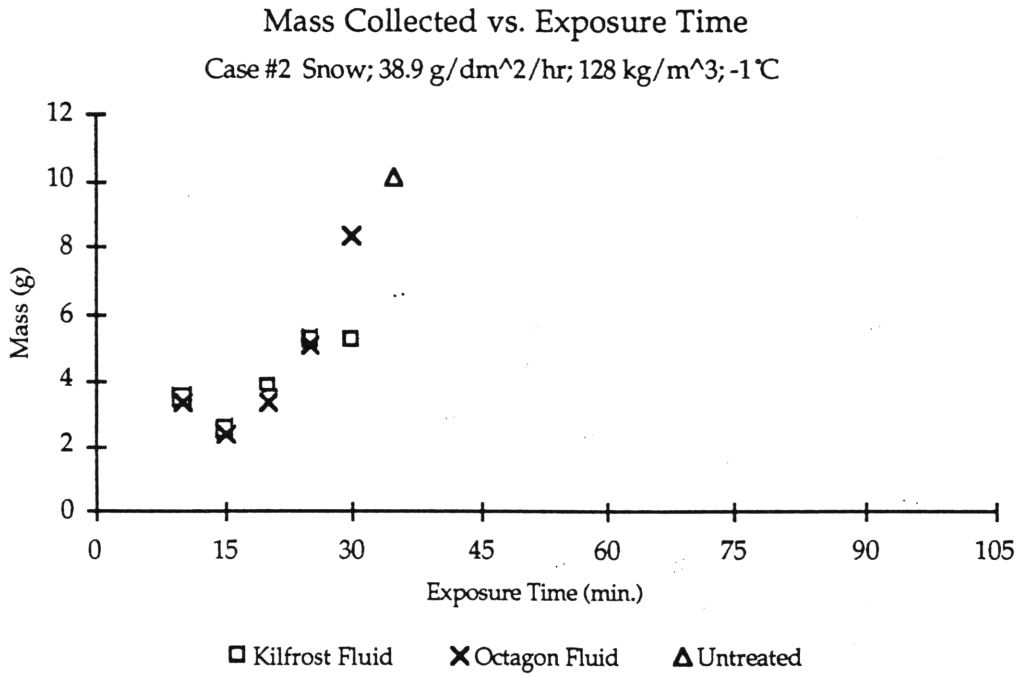

Figure 4.11: Case #2: Mass Collected versus Exposure Time

Similar masses were collected for each fluid. As in Case 1 the collected mass

decreased initially, then increased. Precipitation accumulation occurred faster, as expected due to the higher precipitation rate, which resulted in a steeper curve. At 15 minutes exposure time the mass was at minimum for both plates. Any additional mass past this point consisted of precipitation only, since no fluid was introduced once the exposure started.

The data point for Kilfrost fluid at 30 minutes did not follow the trend. Some fluid or part of the contamination layer might have slid off while mounting the plate on the shear rig.

4.4.3 Case 2: Adhesion

The first set of exposure test plates were spun after 10 minutes and then at 5 minute intervals. At the end of the sequence the untreated control plate was spun.

Minor roughness was evident along the upper edge of both test plates after an exposure time of 10 minutes. Ripples formed in the fluid at about 100 rpm and the fluids were observed to flow off both test plates at this speed.

Fifteen minutes into the event roughly 40% of both test plates were covered by contamination. Again the behavior of the contamination layer on both plates was similar. The contaminated layer near the upper edge started sliding down at a speed of approximately 100 rpm. Ripples in the fluid were visible and the contamination appeared to slide off smoothly along with the fluid in an almost continuous mass.

After an exposure time of 25 minutes, coverage was above 80 percent for both plates. The lower quarter of the Kilfrost plate was clear before a speed of 100 rpm was reached. Slightly above 100 rpm the remaining contamination slid off the plate within a couple of revolutions. No break-up of the contamination layer was observed, instead the layer appeared to slide off as a continuos mass.

Below 100 rpm the lower edge of the contamination layer on the Octagon

plate appeared to break-up. The upper edge had still not moved at 100 rpm, but around 120 rpm the entire remaining contamination moved off as a continuous mass in a couple of revolutions.

A similar behavior was observed on the plates spun 5 minutes later. Both plates were almost completely covered by contamination. The contamination layer slid off suddenly as a continuous mass at around 100 rpm.

The snow layer on the untreated control plate slid off as a continuous mass at a speed of 150 rpm. All the test plates in Case 2 were completely clear after the shear test.

Figure 4.12 and figure 4.13 show the coverage and adhesion versus exposure time for Case 2.

The shear stress required to clear the treated plates remained at the same low level even at full coverage, i.e. no adhesion failure was observed. It seems counter intuitive that no adhesion failure was observed with the higher rate of precipitation in this Case. A possible explanation is that the rapid build-up of contamination did not allow the precipitation enough time to penetrate the fluid layer and thus a fluid layer was present beneath the contamination layer. The observations of the sliding process indicated that this was the case. The VCR failed during the 20 minute spin making it impossible to estimate coverage and adhesion for that time.

The untreated control plate was spun after 35 minutes. A high shear stress was required to remove the snow layer. In this case treating the plates was clearly beneficial.

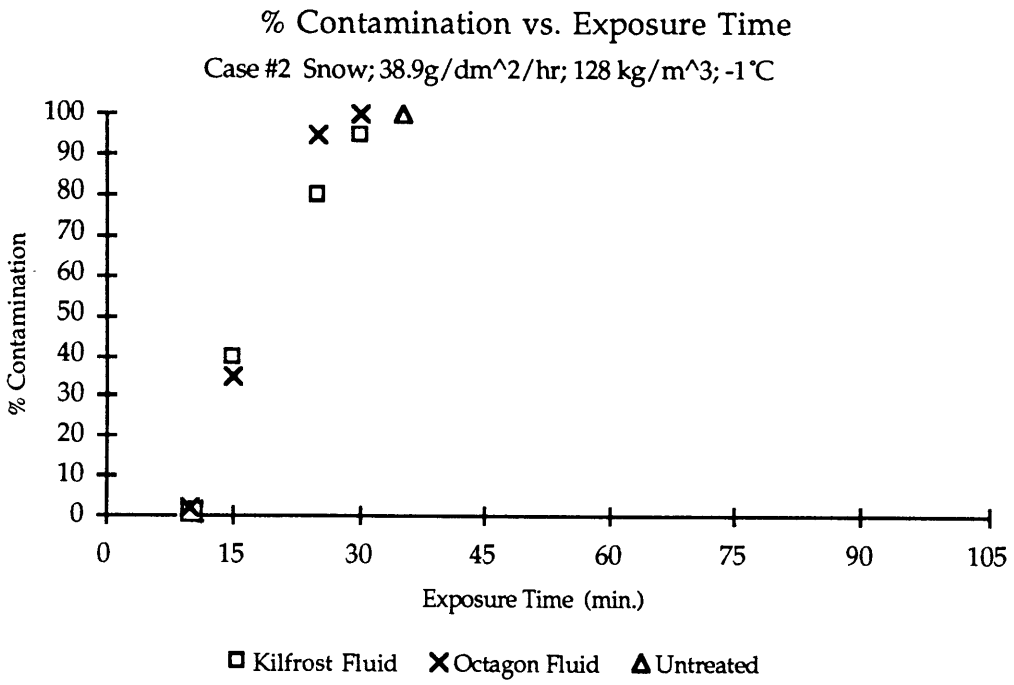

Figure 4.12: Case #2: % Contamination versus Exposure Time

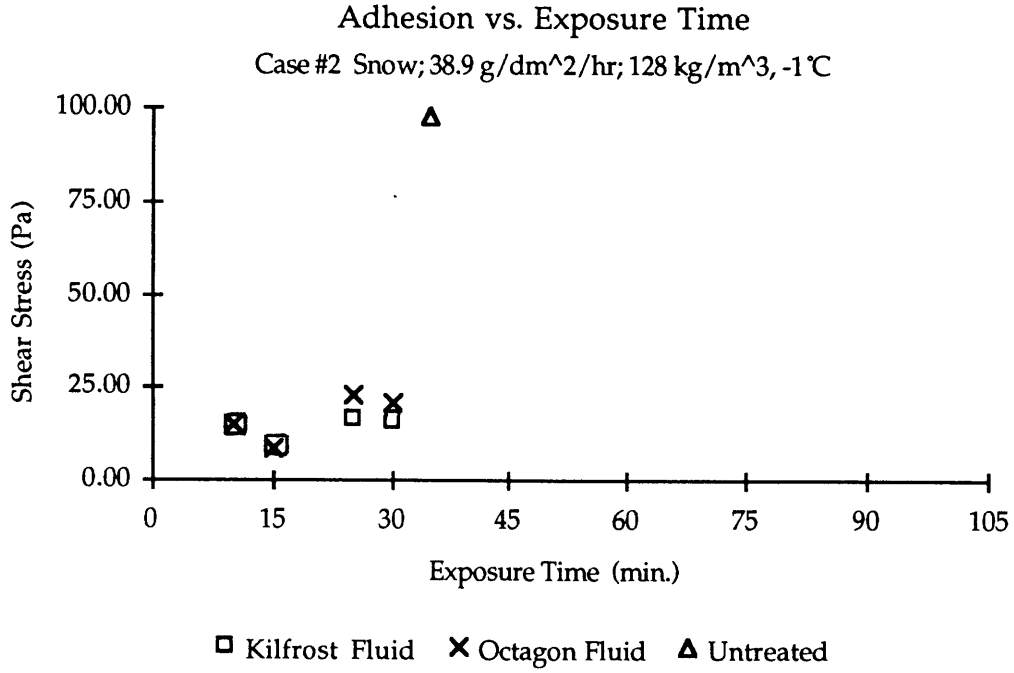

Figure 4.13: Case #2: Adhesion versus Exposure Time

4.5 Case 3: Light Snow, Very Small Flakes

4.5.1 Case 3: General Description

Case 3 was tested during the morning of February 27, 1995. The test plates were treated with undiluted (neat) de-icing fluids. The snow was light (0.5" per hour) and dry (48 kg/m^3) and consisted of very small snow flakes, almost snow grains. The LEPR was calculated to be 6.0 g/dm/hr based on a time period of one hour. The temperature was measured at -6.8°C at 9: 53 am and dropped to -8.3°C in one hour. Initially the snowfall rate increased, however, towards the end of the exposure it stopped snowing.

4.5.2 Case 3: Contamination

Figure 4.14 shows the % contamination coverage of the test plates versus the exposure time. As in the case with a similar precipitation rate (Case 1) the contamination of the plates appeared to occur in three phases.

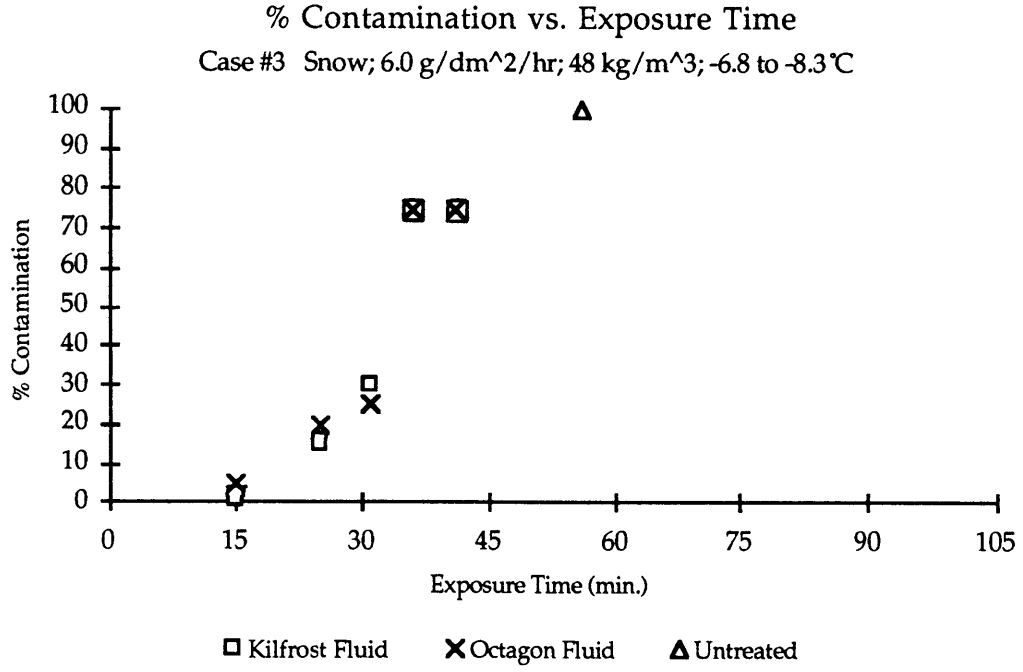

Figure 4.14: Case #3: % Contamination versus Exposure time

The onset of the first slow phase occurred after fifteen minutes for both fluids. Again covering of the majority of the plate happened very sudden. In this case the precipitation ceased and thus full coverage was never reached. There was therefore no evidence of the third phase, but there is no reason to suspect it would not have occurred.

The progression of the contaminated layer in this case was similar to that in Case 1. Contamination appeared along the upper edge and spread down the plate along a line parallel to the upper edge as the exposure time increased.

The observed differences between the contamination of the two fluids were not significant in this case.

Figure 4.15 shows the masses collected during the shear test for Case 3. The collected mass increased only slightly with longer exposure time. This is thought to be due to the addition of precipitation being balanced by the fluid runoff.

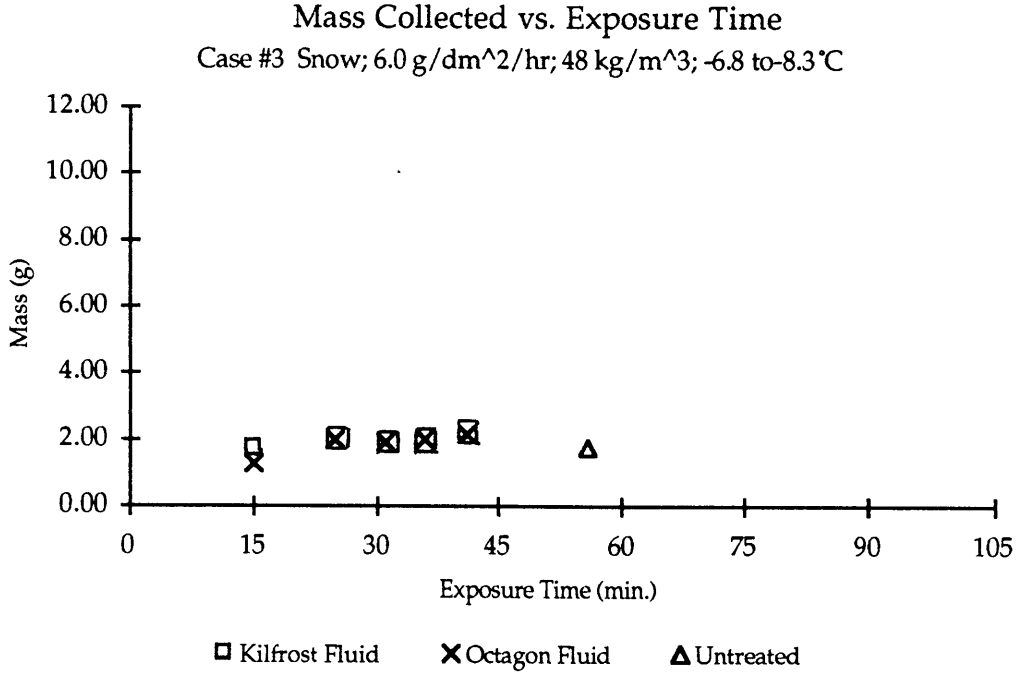

Figure 4.15: Case #3: Mass Collected versus Exposure Time

4.5.3 Case 3: Adhesion

Accumulation was visible after 15 minutes at which time the first set of plates were spun. The next set of plates were spun 10 minutes later with the remaining plates spun at shorter 5 minute intervals due to the increased snow fall rate.

Only minor roughness along the upper edge was visible on Kilfrost plate after 15 minutes exposure time. The upper edge of the plate was observed to be clear of fluid at a speed of 150 rpm. Ripples were observed in the fluid along the bottom edge at a lower speed. The Octagon plate had about 5 % contamination coverage. The fluid layer and most of the contamination except for minor spots on the upper edge cleared off the plate. The contamination was observed to break up and slide down in discrete small lumps.

Twenty-five minutes into the event the coverage of the Kilfrost plate and the Octagon plate was 15 and 20% respectively. At a speed of about 100 rpm fluid and roughness below the 15% line had slid off the Kilfrost plate. The contamination above this line was observed to slide down in discrete lumps at a speed of 150 rpm. Only minor roughness spots were left on the upper edge. The fluid layer below the 50% line on the Octagon plate was observed to slide off around 150 rpm, but no movement of the contamination layer was apparent at this speed. At a speed of 175 rpm the plate appeared to be clear above the 25% line. At 200 rpm there appeared to be less contamination left on the plate, but it was impossible to see any contamination in transition. The image of the plate after the shear test showed some amount of residue in the center of the plate at the 25 % line where the contamination was observed to be heavy. The fluid appeared to drain off before the contamination started sliding leaving behind dry looking contamination and a non-lubricated sliding surface.

A similar process seemed to take place on the plates spun after an exposure time of 36 minutes. The coverage on both plates had increased to around 25 to 30 %. The lower edge of the contamination layer was observed

to break-up at around 200 rpm on the Kilfrost plate. At about 300 rpm the contamination layer near the upper edge was observed to break-up and move down the plate. The plate appeared fairly dry and the contamination did not move down in a smooth manner. The image of the plate afterwards showed roughness down to the 25% line and adhesion failure was determined to have occurred based on this fact. The Octagon plate went through a similar process at about the same speeds. An amount of residue was left on the plate.

Forty-one minutes into the event the contamination coverage remained at 75% on both plates. The fluid near the bottom edge on the Kilfrost plate was observed to form ripples and flow off at a speed slightly above 100 rpm. At 150 rpm contamination up to the 50% line was observed to break-up and flow off, however there were spots below this line where the contamination did not move at all. Close to 300 rpm the lower two thirds of the plate appeared clear, but contamination on the upper part of the plate remained continuous. The image of the plate afterwards showed residue on the upper part of the plate with more in the spots where the contamination layer appeared to be thickest. The contamination below the 75% line on the Octagon plate started to break-up around 125 rpm. The loosened contamination slid off the plate in large lumps. Close to 200 rpm the contamination layer was breaking-up in a line across the plate at the halfway point. As the speed increased the contamination up to the 20% line started to flow down a few paths. The image after the shear test showed a fairly continuous thin layer of residue above the 25% line and smaller spots below. The residue appeared very dry.

The untreated control plate was spun after 56 minutes. The lower half off the snow layer cleared of at a speed close to 150 rpm. The upper half slid off in two big continuous lumps of mass at a speed of 250 rpm.

Figure 4.16 and 4.17 show the coverage and adhesion versus exposure time respectively. In this Case a large jump in the shear force was observed at low levels of contamination, which indicated adhesion failure had occurred. For both fluids only about a third of the plate was contaminated at the time of adhesion failure. Adhesion failure was observed sooner for Octagon fluid, at about 25 minutes. The arrows indicate that the required acceleration was above the maximum motor limit, i.e. the plates did not clear completely.

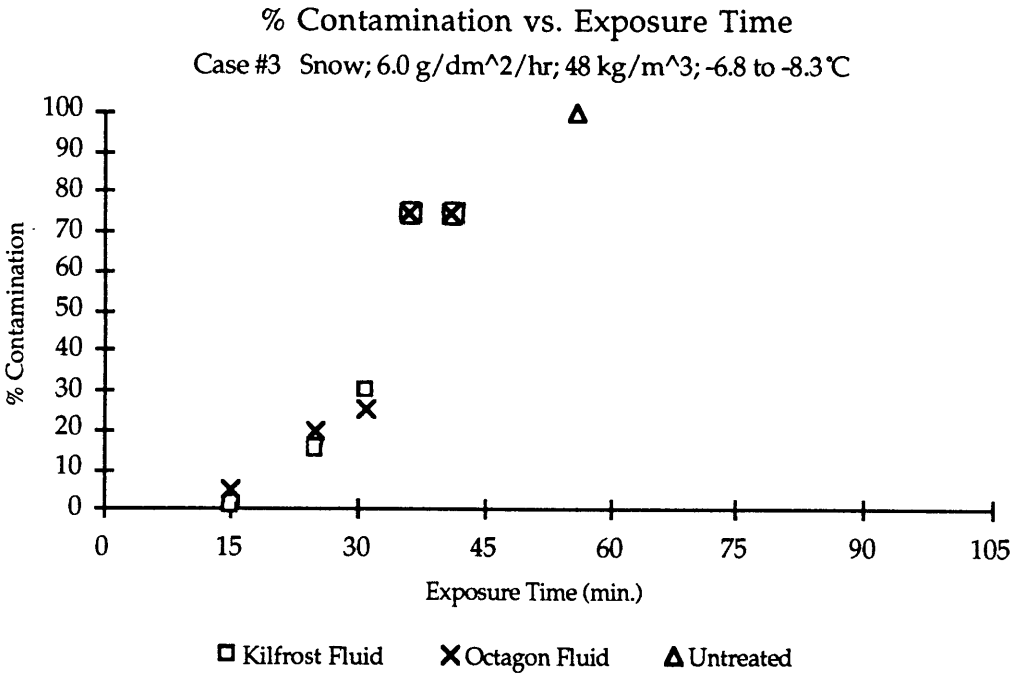

Figure 4.16: Case #3: % Contamination versus Exposure time

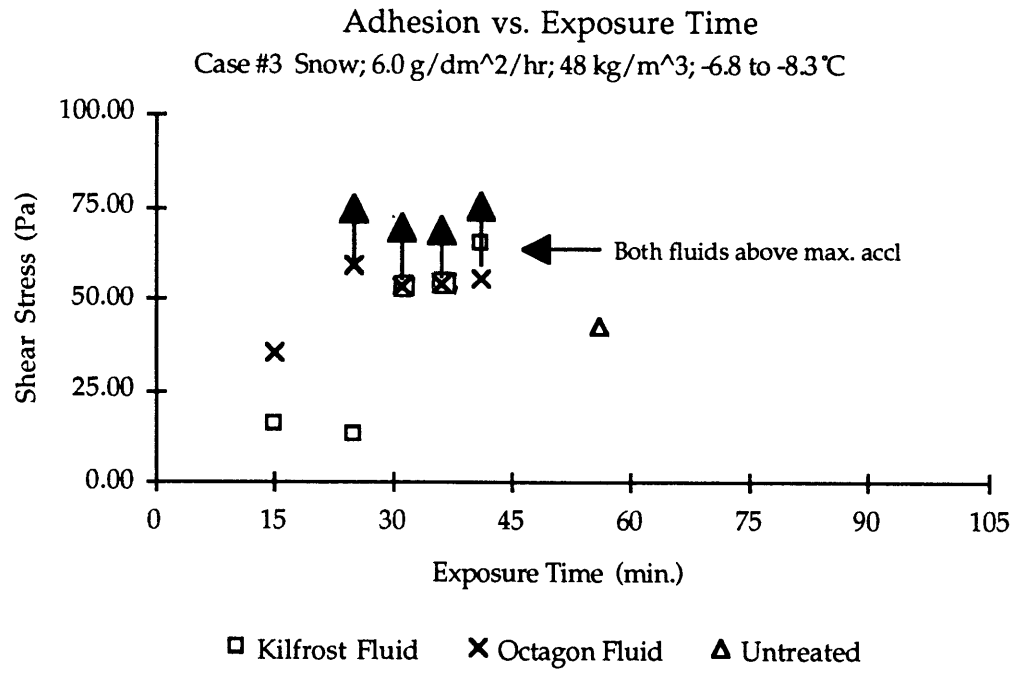

Figure 4.17: Case #3: Adhesion versus Exposure Time

The untreated control plate was spun after 56 minutes at which time it was completely covered. The shear stress required to clear the snow layer off was lower than the stress required for the treated plates.

4.6 Case 4: Light Freezing Rain

4.6.1 Case 4: General Description

The data for Case 4 were also obtained on February 27. The precipitation changed to light freezing rain during the afternoon. The temperature recorded at 4:45 PM was -1.5°C, but it dropped to -6.7°C by 5:23 PM. The density of the freezing rain was calculated to be 243 kg/m^3 with a LEPR of 5.9 g/dm/hr. The precipitation rate decreased during the experiment with the precipitation ceasing before full coverage was observed. As in the previous tests the test plates were coated with undiluted de-icing fluids.

4.6.2 Case 4: Contamination

The estimated contamination coverage of the plates is shown in figure 4.18. It was generally harder to estimate the percentage of the total area contaminated in this Case because the contamination area was not continuous and consisted mostly of early intermediate stage (roughness) contamination. The area of contamination did not show a continuous increase with time, since the precipitation rate decreased during the exposure.

In this case no pattern of phases were apparent. The process of contamination in this case was different from the process observed in the snow cases. Rough spots appeared soon after fluid application. The rough spots were located mostly on the upper half of each plate. The observations showed that the roughness did not proceed down the plates in a regular manner, but occurred in spots with increasing density up the plate. Towards the end of the event the precipitation rate had decreased which resulted in decreased contamination on both plates. Based on the observations no significant difference between the two fluids was apparent.

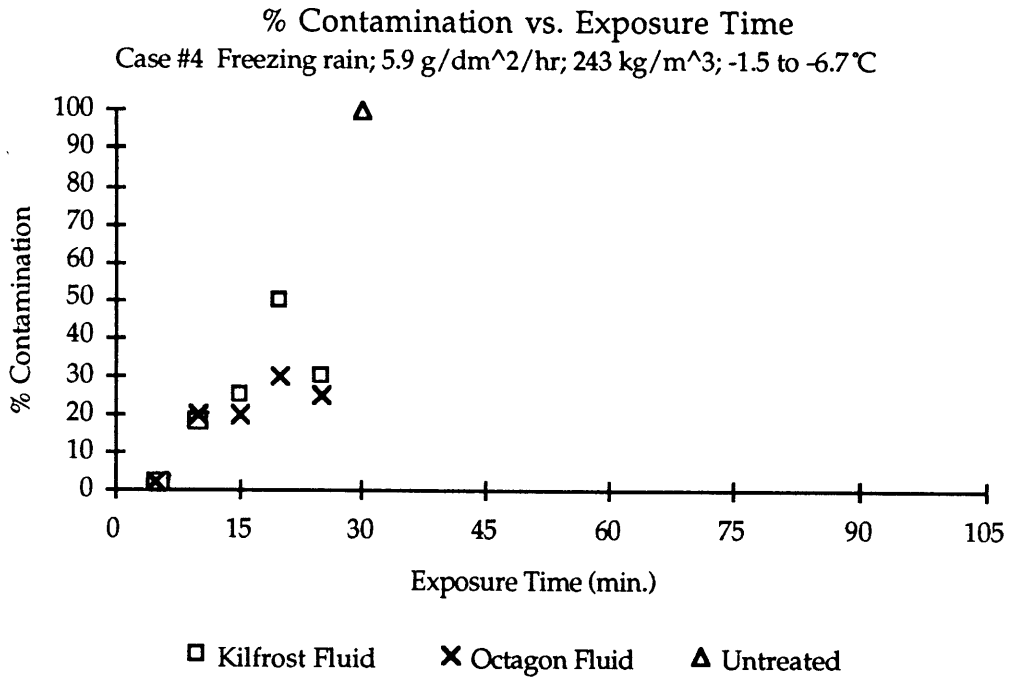

Figure 4.18: Case #4: % Contamination versus Exposure Time

Figure 4.19 shows the collected mass for Case 4.

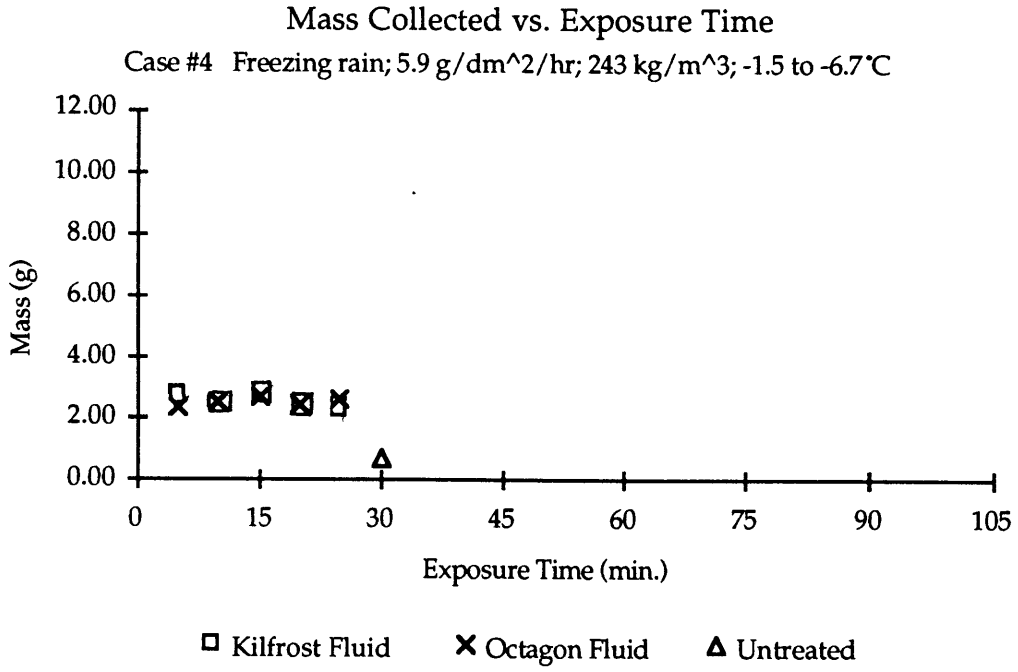

Figure 4.19: Case 4: Mass Collected versus Exposure Time

The mass did not change much with exposure time. This is thought to be due to the interaction of the precipitation with the fluid film. The observations showed that not all rain droplets mixed with the fluid film, but instead formed water pools at the top of the fluid. The top layer of water appeared to run off the plate during the exposure. This phenomenon could account for the lack in increase of the collected mass.

4.6.3 Case 4: Adhesion

The first set of plates were spun after 5 minutes when accumulation became visible. Subsequent spins were done at 5 minute intervals.

The quality of the video of the test plates at 5 minutes was not good enough to allow a determination of the speed at which sliding occurred. However, both plates were clear afterwards. The behavior of the contamination layer on both test plates was similar for subsequent test plates in this shear test. At a low speed ripples would form in the fluid and runoff would start at the lower edge. As the speed increased contamination and fluid higher up on the plate would start to flow off. The speed at which contamination close to the upper edge started to move down increased slightly with the exposure time. The test plates were clear after spinning except for minor residue at the upper edge of the plates.

The untreated control plate was spun after 30 minutes. The precipitation layer on this plate did not move at all, but appeared as a glazed surface on the plate.

Figure 4.20 and 4.21 show the coverage and adhesion data for the freezing rain case. The data for 5 minutes have not been included due to poor quality. The glare from the strobe light made it impossible to accurately estimate the coverage and the acceleration at sliding.

The adhesion data were somewhat scattered, but a trend of increasing adhesion with time was apparent. No large jump in shear stress values was observed for the test plates in this Case, i.e. adhesion failure was not observed.

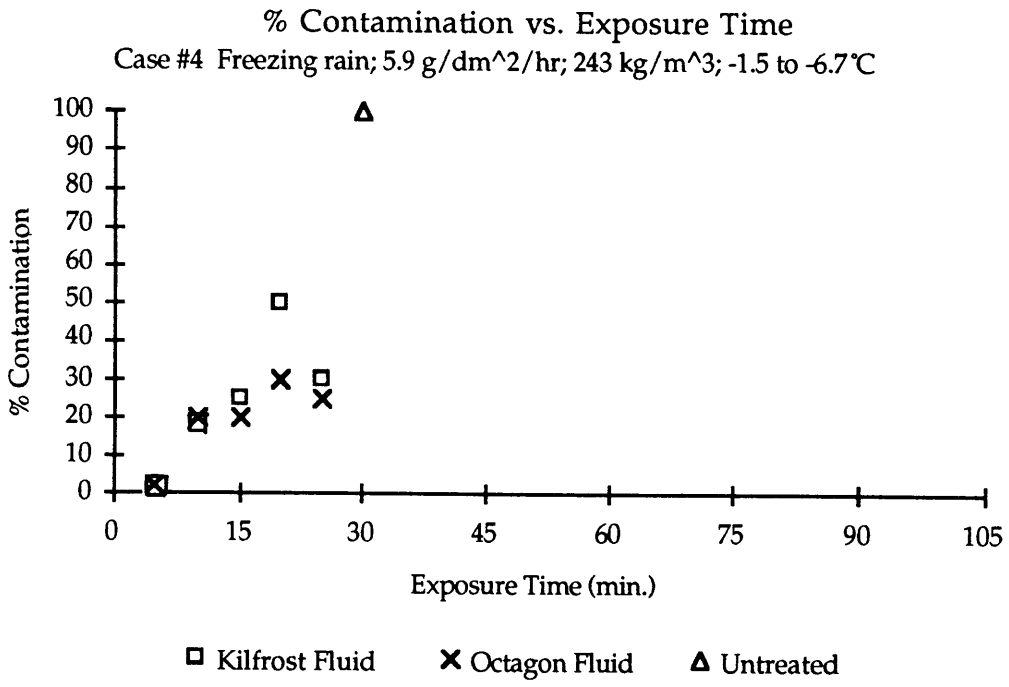

Figure 4.20: Case #4: % Contamination versus Exposure Time

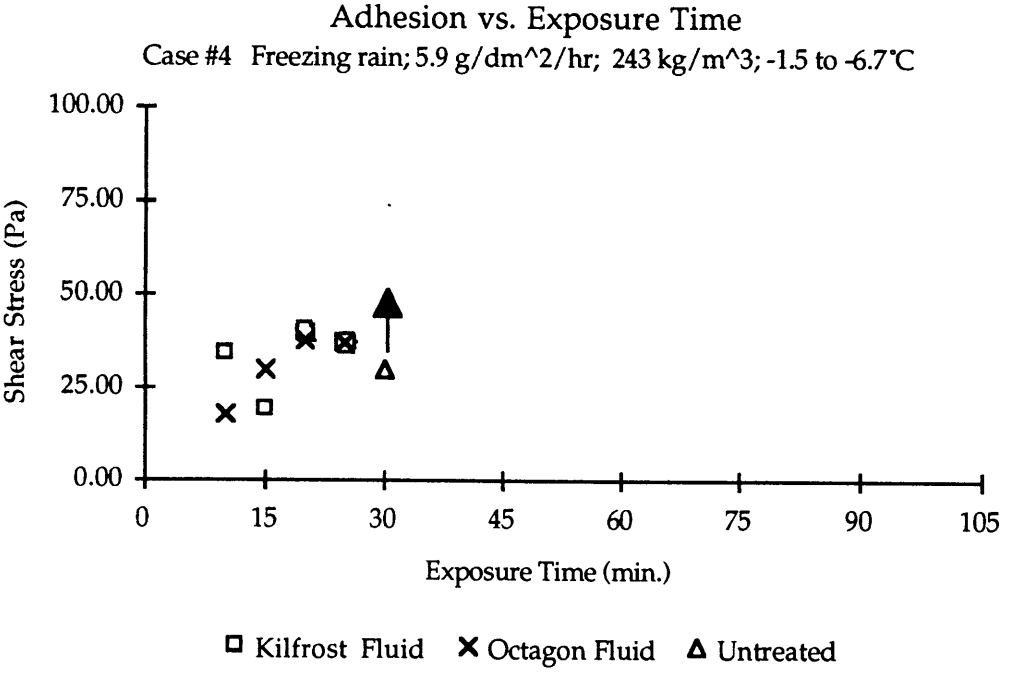

Figure 4.21: Case #4: Adhesion versus Exposure Time

However, the shear analysis method used for calculating the adhesion force did not apply particularly well to the freezing rain case. The assumption that the shear element slides as a continuous mass was not accurate for this case and thus the results should be taken with some caution.

The untreated plate was completely covered by a rough ice layer after 30 minutes. This ice layer did not slide during spinning at the maximum motor acceleration. Thus for the case of freezing rain, and the specific environmental conditions, treating the plates provided a significant improvement.

Chapter 5

Observed Failure Modes

The observations of the contamination process and the shear process indicated the existence of two distinct failure modes. The type of failure mode appeared to influence the shear stress that was required to clear the test surface of the contamination layer. It is thought that the two types of failure modes are caused by different interactions of the precipitation with the fluid layer. The environmental conditions were observed to affect these interactions. The details of the two failure modes are presented in this chapter.

5.1 Bridging Failure Mode

The bridging failure mode is named so because the contamination elements appeared to form a bridge on top of the fluid. Figure 5.1 shows a schematic of the fluid-precipitation layer with bridging failure mode.

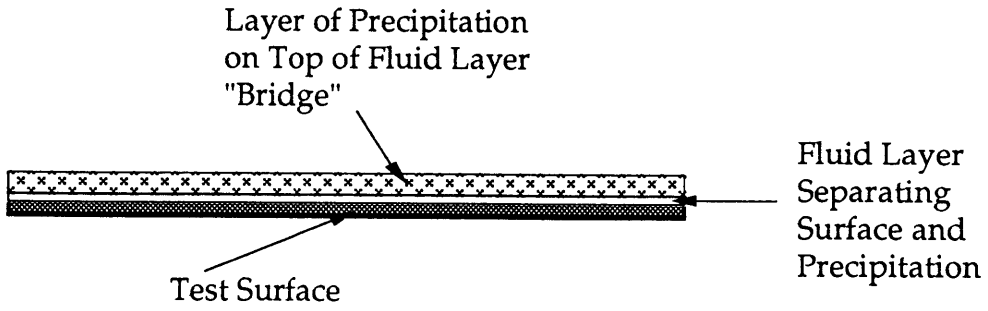

Figure 5.1 Fluid-Precipitation Layer with Bridging Failure Mode

This failure mode was observed in the snow case that had a high precipitation rate and a temperature just below freezing. In this case the contamination progressed rapidly once the roughness became visible along the upper edge. The relatively short time before contamination was observed and the short coverage time associated with the high precipitation rate appeared to prevent the precipitation elements from penetrating the fluid, leaving a fluid layer beneath the contaminated layer.

The observations of the sliding process showed that the contamination layer sheared off fast and smoothly in one or two lumps of continuous mass when low shear was induced. An example of this is given in figure 5.2 below.

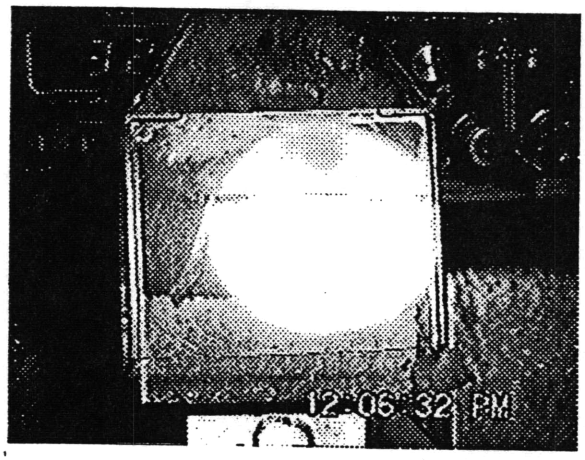

Figure 5.2: Contamination layer ,showing bridging failure mode, sliding off the test surface. (Case 2 - high precipitation rate)

This observation supports the idea of a fluid layer separating the test surface and the contamination layer. With a fluid layer beneath the adhesion is low which reduces the shear stress required to clear the plate of contamination.

5.2 Penetration Failure Mode

The penetration failure mode was observed in the two snow cases that had low precipitation rates (Case 1 & Case 3). In these two cases the onset of contamination occurred later than in Case 2, allowing some of the precipitation elements time to penetrate the fluid layer. Figure 5.3 shows a schematic

of the fluid-precipitation layer with penetration failure mode.

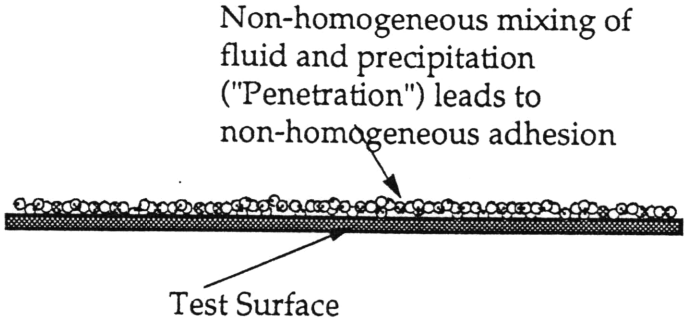

Figure 5.3 Fluid-Precipitation Layer with Penetration Failure Mode

The contamination process consisted of three phases of which the middle phase is more interesting, since the other two can be attributed to edge effects. In the second phase the majority of the plate was contaminated in a short time.

In these two cases the interaction of the fluid elements with the fluid layer is thought to consist of non-homogeneous mixing. The non-homogeneous mixing would result in a non-homogeneous adhesion process. This non-homogeneous adhesion process were evidenced by the break up of the contamination layer that was observed in these two cases. An example of this, for Case 1, which had low precipitation rate and a temperature just below zero, is shown in figure 5.4.

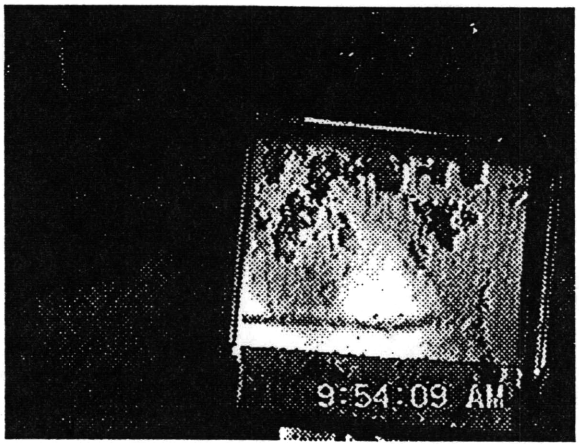

Figure 5.4: Contamination layer breaking up and sliding off the test surface
(Penetration failure mode, Case 1 - low precipitation rate)

Another example of the same process is shown in figure 5.5.

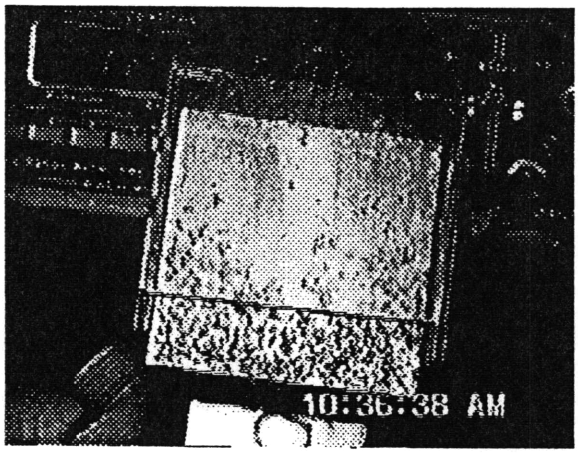

Figure 5.5: Contamination layer breaking up and sliding off the test surface
(Penetration failure mode, Case 3 - low precipitation rate & lower temperature)

This example is taken from Case 3, where the precipitation rate was similar to that in Case 1, but where the temperature was about 5 °C colder. The colder temperature is thought to have the effect of increasing the adhesion force. The observations showed that for this case residue was left on most of the plates, particularly in the areas where the contamination was heaviest.

The shear required to clear the plates in the cases that had low precipitation rate and experienced the penetration failure mode was generally higher than the shear for the case in which a high precipitation rate resulted in bridging failure mode. A combination of low precipitation rate and lower temperature resulted in high levels of adhesion at low levels of contamination coverage.

Chapter 6

Summary and Conclusions

The objective for the research was to perform a detailed study of the failure modes of Type II aircraft ground de-icing fluids exposed to natural precipitation conditions. The study focused on determining if the fluid layer, contaminated by precipitation, adheres to the testing surface. The goal was to identify if a higher level of adhesion was associated with a particular failure mode.

The approach was to experimentally measure the shear force required to clear naturally accumulated precipitation off a surface treated with Type II deicing fluid. Four shear test were carried out during two different snow events. Data sets were obtained for light snow, heavier snow and freezing rain conditions. Video recordings provided close up views of the contamination process and the shear process and allowed a rough estimate of the adhesion.

The limited amount of cases that were studied preclude a general conclusion. However, the observations did seem to indicate the existence of two distinct failure modes. The failure modes appeared to be related to the way the precipitation elements interacted with the fluid layer. A higher precipitation rate was observed to result in a bridging failure mode, where the contamination was separated from the test surface by a fluid layer. In this case the contamination progressed rapidly and abruptly, once the roughness became visible along the upper edge of the test plate. A lower precipitation rate led to penetration of the fluid layer, a three phased contamination process and gen-

erally higher adhesion. The research showed that adhesion failure does occur, is unambiguous and can be tested.

It is recommended that further tests be done, encompassing a greater variety of weather conditions. A more accurate shear analysis method should be developed that would allow analysis of freezing rain cases. A way of determining the composition of the collected contamination layer would be helpful in that respect.

References

Anagnostakis, Ioannis (1994), Experimental Investigations of Physical Factors which Influence Runoff and Failure Behavior of Aircraft De-icing Fluids, Aeronautical Systems Laboratory, Massachusetts Institute of Technology, August 1994.

ARCO Chemical Company, Kilfrost ABC-3 Fluid (Type II), Product Documentation.

Federal Aviation Administration (1982), Advisory Circular AC 20-117, Hazards Following Ground De-Icing Operations in Conditions Conducive to Aircraft Icing, US Department of Transportation, December 17, 1982.

Federal Aviation Administration (1992), Advisory Circular AC 120-58, Pilot Guide Large Aircraft Ground Deicing, US Department of Transportation, September 39, 1992.

Federal Aviation Regulations (1994), Jeppesen Sanderson, Inc., 1994.

Haase D.J. (1991), Aircraft Ground De-icing, A flight Crew Perspective. 29th Aerospace Sciences Meeting, AIAA paper 91-0761, 1991.

Masters, C.O.(1991), Aircraft Ground Deicing, SAE technical paper series, AIAA paper # 912222, 1991.

Octagon Process Inc., Octagon Forty Below Aircraft Wing Anti-icing De-icing Fluid (Type II), Product Documentation.

Ross, F. (1991), The Contrasting Requirements for Type II De-/Anti-Icing Fluids, AIAA paper # 91-0759, 1991.

Appendix A Runoff Data for Kilfrost and OctagonFluid

Runoff vs. Time (No precipitation)
Curve fit for Kilfrost Fluid

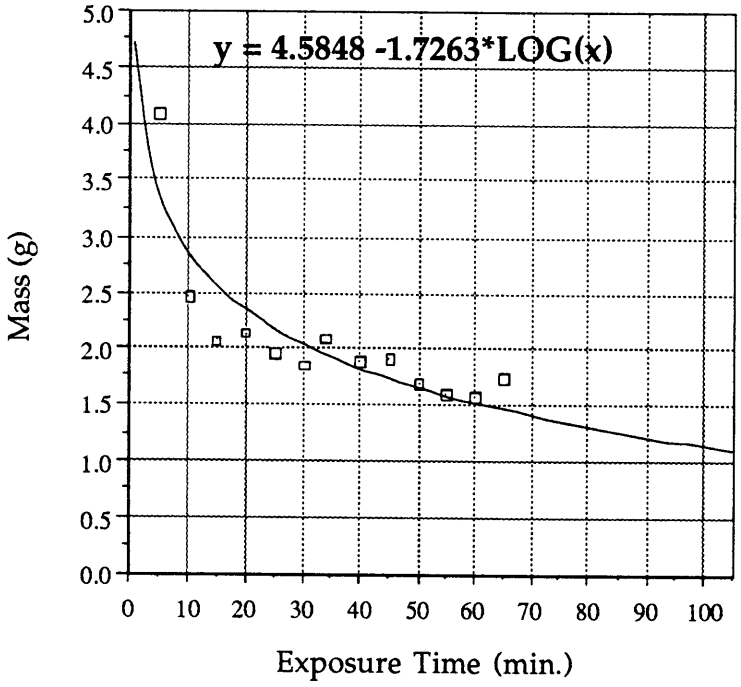

Runoff vs. Time (No precipitation)
Curve fit for Octagon Fluid

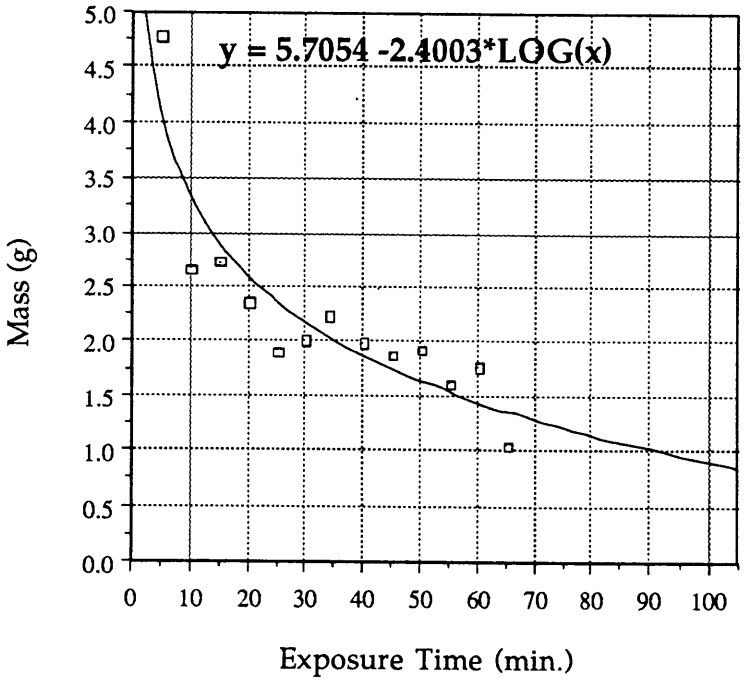

Appendix B Shear Data for Kilfrost and Octagon Fluid

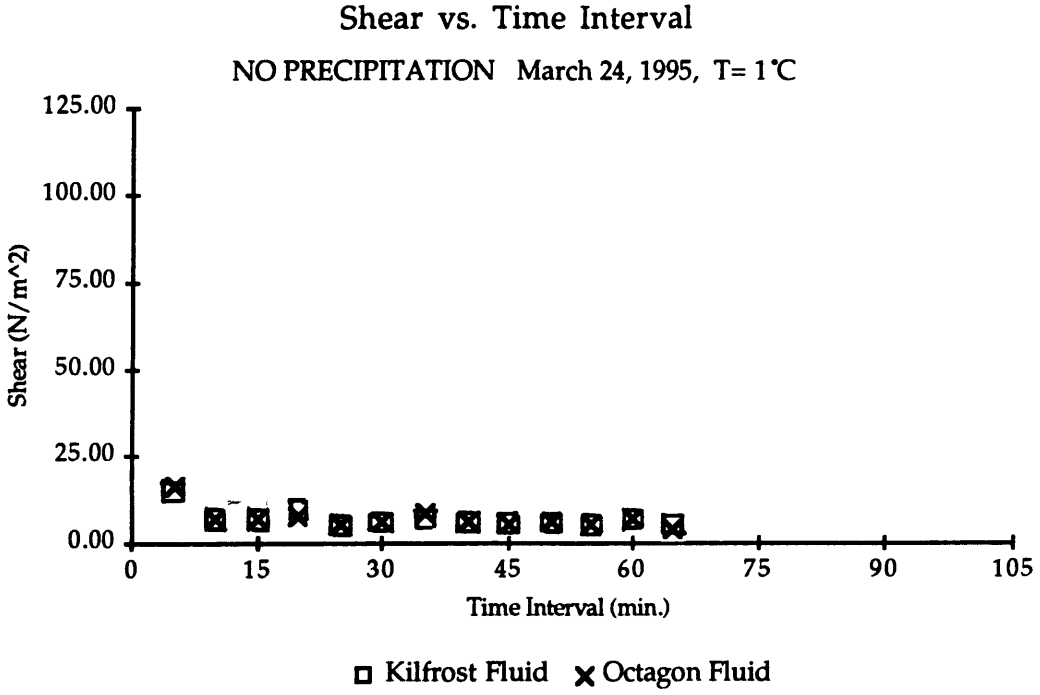

The shear was seen not to vary substantially with the time interval. A shear of about 10 Pa was sufficient to clear the test plate of de-icing fluid. However, a very thin film of fluid did remain on the surface.